BROOKHAVEN NATIONAL LABORATORY
Associated Universities, Inc.
Upton, L.I., N.Y.

JRS/CLW-1

ACCELERATOR DEPARTMENT
AGS
INTERNAL REPORT

EMPIRICAL FORMULAS FOR PARTICLE PRODUCTION IN P-Be COLLISION BETWEEN 10 AND 35 BeV/c

J.R. Sanford and C.L. Wang

March 1, 1967

Introduction

The purpose is to construct empirical formulas which give quantitative representations of the secondary particle production in P-Be collision, based on the characteristics of the experimental data between 10 and 34 BeV/c incident proton momenta. Except for certain kinematical constraints, the approach is, therefore, purely algebraic rather than physical.

Part I - Pion Production

1. Angular Dependence of the Momentum Spectra

The angular dependence of the momentum spectra can be studied by taking the ratio of the production at angle θ to the forward production. An example is shown for positive pions in Fig. 1 at 18.8 and 23.1 BeV/c incident proton momenta, by utilizing the data of Dekkers et al.[1] Call this ratio g, we see that on the semi-log plot, g is well represented by a linear function whose slope h is apparently independent of the incident momentum. Clearly g crosses unity at some value P_c of the secondary momentum P. (Note $P_c \neq 0$). Similar investigation was made at 13.4 BeV/c, based on the data of Lundy et al.[2] Though there is no measurement of the forward production at this momentum, the detailed data enable a fairly dependable extrapolation to zero degree. The

study of the behavior of g at 13.4 BeV/c supports the observation at 18.8 and 23.1 BeV/c; namely, the slope h is independent of the incident momentum P_i, and is a function of the production angle θ alone. Assuming this to be true at 30 BeV, we thus obtain an expression

$$g = e^{-h(\theta)\ (P-P_c)} \qquad (1)$$

Now h has to vanish at $\theta = 0$, where g reduces to 1. Furthermore, the data at 13.4 BeV/c indicate that P_c decreases as θ increases, while the data at 18.8 and 23.1 BeV/c show that P_c increases as the incident momentum increases. To accommodate these features we chose the functional forms

$$h = a\ \theta^m \qquad (2)$$

$$P_c = b\ P_i\ \cos^n\theta \qquad (3)$$

where a, b, m, and n are unknown constants to be determined by the least square analysis.

2. Forward Production

The general characteristics of the forward production as observed on the semi-log plot are:

1. The momentum spectrum decays with a power greater than one.
2. The higher the incident momentum, the slower the decay of the momentum spectrum, and
3. The momentum spectrum has a maximum and decreases rapidly as the secondary momentum approaches zero.

In addition to these characteristics, the momentum spectrum has to satisfy a certain kinematical requirement, namely

4. The spectrum must vanish as the secondary momentum reaches the incident momentum, (slightly below the incident momentum, to be exact). To satisfy above features, we assume for the forward production spectrum the functional form

$$f = C_1 P^{C_2} \left(1 - \frac{P}{P_i}\right) e^{-\frac{C_3 P^{C_4}}{P_i^{C_5}}} \qquad (4)$$

where C_1 through C_5 are unknown constants to be determined.

3. Least Square Analysis

Combining the forward production f and the angular dependent term g, we have the complete double differential momentum spectrum

$$\frac{d^2N}{d\Omega dp} = f.g$$

$$= C_1 P^{C_2} \left(1 - \frac{P}{P_i}\right) e^{-\frac{C_3 P^{C_4}}{P^{C_6}}} - C_6 \theta^m \left(P - C_7 P_i \cos^{C_8} \theta\right) \qquad (5)$$

where C_1 through C_8 and m are the parameters to be determined by the least square fitting to the experimental data (m turned out to be 1). The data used in the analysis are from four experiments; by Lundy et al., at 13.4 BeV/c[2], Dekkers et al., at 11.8, 18.8 and 23.1 BeV/c[1]; Baker et al., at 10.9, 20.9 and 30.9 BeV/c[3] and Fitch et al., at 33.9 BeV/c[4].

A. Normalization of the Experimental Data

In view of the relatively limited experimental data, every bit of them is of great value. The data of Lundy et al. cover most thoroughly the detailed angular dependence of the momentum spectrum, and are thus invaluable in determining the function h (θ), while the data of Dekkers et al. are the sole data which present the forward productions and are particularly useful in determining the function f. The data of Baker et al. on the other hand, covered the largest range of the incident momentum. Thus all data complement each other and are essential in determining the complete momentum spectrum. However, in order to take full advantage of all available data from different experiments with completely different experimental setup, care must be taken in their relative normalization. We have chosen the data of Dekkers et al., as the standard of normalization.

The experiment of Baker et al. and that of Fitch et al. were performed with an internal target of which the efficiency was quoted as $\eta = 50 \pm 10\%$. Considering the momentum dependence of the target efficiency, we assumed $\eta = 50$, 53 and 60% at $P_i = 10.9$, 20.9 and 30.9 and 33.9 BeV/c respectively. Because of the uncertainties of these efficiencies and the uncertainties of the effect of the AGS fringe field on the secondary particles, relatively large errors (20%) were assigned to the experimental data. Whether further normalization relative to the data of Dekkers et al. is necessary or not will be found in the least square analysis.

The normalization of the data of Lundy et al. was checked in two ways. First, the forward production spectra of $\pi^{\pm}$ and protons at 13.4 BeV/c were obtained by extrapolating the data to zero degree, and were then compared with the corresponding forward production spectra of Dekkers et al. at 11.8, 18.8 and 23.1 BeV/c. Secondly, various normalization factors were assumed and least square analyses were carried out with all other experimental data ranging from 11 to 34 BeV/c. Both results are consistent with a normalization factor of 1.5 to be multiplied to the data of Lundy et al. The errors assigned to these data in the least square analysis were 15%.

In converting the unit from (mb/nucleus) to (number of pions/interacting proton), the absorption cross section σ_a was taken to be 227 mb[5]. To summarize, the data from different experiments were normalized and the units were converted by

$$\frac{d^2N}{d\Omega dp} \quad \text{(number of pions/sr/BeV/c/interacting proton)}$$

$$= \frac{N_L}{\sigma_a} \left(\frac{d^2\sigma}{d\Omega dp}\right)_{\text{Lundy et al.}} \quad \text{(mb/sr/BeV/c/nucleus)} \qquad (6)$$

$$= \frac{1}{\sigma_a} \left(\frac{d^2\sigma}{d\Omega dp}\right)_{\text{Dekkers et al.}} \quad \text{(mb/sr/BeV/c/nucleus)}$$

$$= \frac{N_B}{\eta} \left(\frac{d^2N}{d\Omega dp}\right)_{\substack{\text{Baker et al.} \\ \text{Fitch et al.}}} \quad \text{(number of pions/sr/BeV/c/circulating proton)}$$

where N_L (=1.5) and N_B are the normalization factors for the data of respective authors, and η_i is the efficiency of the internal target. N_B turned out to be $\sim$ 1 with the choice of η_i mentioned before.

B. Least Square Analysis

The Fortran program "LEAST"[6] was used to determine the parameters C_1 through C_8 and m, by minimizing the quantity

$$Q = \frac{1}{F} \sum_i \left[\frac{\log \left(\frac{d^2N}{d\Omega dp}\right)^e_i - \log \left(\frac{d^2N}{d\Omega dp}\right)^c}{\Delta\left(\frac{d^2N}{d\Omega dp}\right)^e_i \Big/ \left(\frac{d^2N}{d\Omega dp}\right)^e_i} \right]^2 \qquad (7)$$

where the superscript e and c refer to the experimental and calculated values respectively, $\Delta \left(\frac{d^2N}{d\Omega dp}\right)^e_i$ is the error pertaining to the i-th experimental datum and F is the number of degrees of freedom in the least square fitting. Good fits were obtained for both π^+ and π^- data with m consistent with 1. Consequently m was set to 1 and equally good fits were obtained with the following parameters.

	C_1	C_2	C_3	C_4	C_5	C_6	C_7	C_8	data	Q
π^+	1.092	.6458	4.046	1.625	1.656	5.029	.1722	82.65	134	0.72
π^-	0.821	.5271	3.956	1.731	1.617	4.735	.1984	88.75	152	0.73

The calculation was done by CDC-6600 and the results were plotted by the CAL-COMP plotter by means of the Fortran program "YIELD" written for this purpose. They are reproduced in Fig. 2 through Fig. 19. The fact that no normalization for the data of Baker et al. was necessary indicates that our assignment of the target efficiency is probably not far from reality.

4. Multiplicities, Mean Secondary and Transverse Momenta, and Inelasticities.

In addition to the momentum spectra, an important experimental observable

that can provide a direct check to the validity of the formula is the pion multiplicities N_π, defined by

$$N_\pi = \int_0^{P_i} \int_0^{\pi} 2\pi \frac{d^2N}{d\Omega dp} \sin\theta d\theta dp \qquad (8)$$

Other quantities of interest are the mean secondary momentum $\bar{p}$, mean transverse momentum P_t and the inelasticities K_π defined respectively by

$$\bar{p} = \frac{1}{N_\pi} \int_0^{P_i} \int_0^{\pi} 2\pi \frac{d^2N}{d\Omega dp} p \sin\theta d\theta dp \qquad (9)$$

$$P_t = \frac{1}{N_\pi} \int_0^{P_i} \int_0^{\pi} 2\pi \frac{d^2N}{d\Omega dp} p \sin^2\theta d\theta dp \qquad (10)$$

and

$$K_\pi = \frac{1}{P_i} \int_0^{P_i} \int_0^{\pi} 2\pi \frac{d^2N}{d\Omega dp} p \sin\theta d\theta \qquad (11)$$

The integrations were carried out numerically, and the results are presented in Table I. A comparison of the calculated multiplicities with the experimental measurements is given in Table II (Section 5).

Table I - Pion Multiplicities, Mean Secondary and Transverse Momentum, and Inelasticities Predicted by the Proposed Formula.

	P_i (BeV/c)	N_π	$\bar{p}$	P_t	K_π
π^+	10	0.97	0.82	0.23	.080
	15	1.17	1.14	0.24	.089
	20	1.38	1.46	0.25	.101
	25	1.64	1.77	0.26	.116
	30	1.94	2.06	0.27	.134
	35	2.33	2.32	0.28	.155
π^-	10	0.87	0.70	0.22	.061
	15	1.02	0.95	0.24	.065
	20	1.18	1.22	0.25	.072
	25	1.37	1.50	0.25	.082
	30	1.61	1.77	0.26	.095
	35	1.91	2.02	0.27	.111

5. Discussion and Comments on Previous Formulas

One interesting feature the present analysis revealed is that the power to the production angle θ reduced to one after the least square fitting, despite some indications of the necessity of higher powers called for by various authors.[7,8,9] Furthermore, the coefficient for the term $P\theta$ is independent of the incident momentum. Therefore, in conjunction with the cosmic ray results at higher energies, it can be considered as established that the transverse momentum distribution of secondary pions is independent of the incident proton momentum P_i for $P_i > 10$ BeV/c.

Several empirical formulas for pion productions have so far been proposed. The formula due to Cocconi, Koester and Perkins[10] assumes a Boltzman distribution for the transverse momentum, and a simple exponential for the forward energy spectrum. It is attractive with its elegant and simple assumptions. However, the representation is fairly qualitative between 10 and 34 BeV/c. It is perhaps of special use at higher energies. Von Dardel's formula[7] is also rather qualitative. The formula due to Haberler[11] is reasonably quantitative, but the parameters are discontinuous. The formula of Burns et al.[8] gives good representation at 20 and 30 BeV only with different parameters, therefore, is not suitable for general purpose. Trilling's formula[12] is based on an attractive combination of the philosophies of the statistical and isobar models and presents very impressive bumps on the momentum spectrum at higher energies; however, it still remains relatively qualitative below 30 BeV. A step toward a quantitative representation between 10 and 30 BeV was recently presented by Ranft by means of a ten-parameter formula, yet the prediction of the pion multiplicities still remains quite poor.

A comparison of the predictions of the pion multiplicities from three most recent formulas with the experimental measurements is presented in Table II.

Table II - A Comparison of the Measured and Predicted Pion Multiplicities, $N_{\pi^+} + N_{\pi^-}$.

P_i (BeV/c)	Experiment*	Proposed Formula	Ranft Formula*	Trilling Formula*
10	1.9 - 2.3	1.84	0.82	0.72
15	2.5	2.19	1.32	0.85
20		2.56	1.85	0.95
25	2.9 - 3.7	3.01	2.39	1.04
30		3.55	2.94	1.12

*These items are quoted from Reference 9.

6. Conclusion

Aside from the goodness of fits to the momentum spectrum, the most remarkable achievement of the present formula is perhaps its excellent prediction of the pion multiplicities, with which the previous formulas really did not have much luck. It is conceivable, therefore, that the present formula is definitely more realistic than any hitherto available formulas as far as the quantitative representation of the pion flux from P-Be collision between 10 and 35 BeV/c incident momenta is concerned. Further study and some modification of the formula may enable an extrapolation to a higher energy. Similar study on kaon and antiproton production is quite promising, and the results will appear in Part II of this report before long.

We appreciate Miss Janet Head for programming "YIELD" and other assistances. One of us (CLW) thanks Dr. Rudolph Sternheimer and Dr. George Trilling for useful conversations. The effort of Mr. Fred Kuehl, Mr. Paul Hallowell and Mr. Malcolm McCrum in various stages of the data reduction and analysis is gratefully acknowledged.

JRS/CLW:lsl
Distr: B1, B2, B3

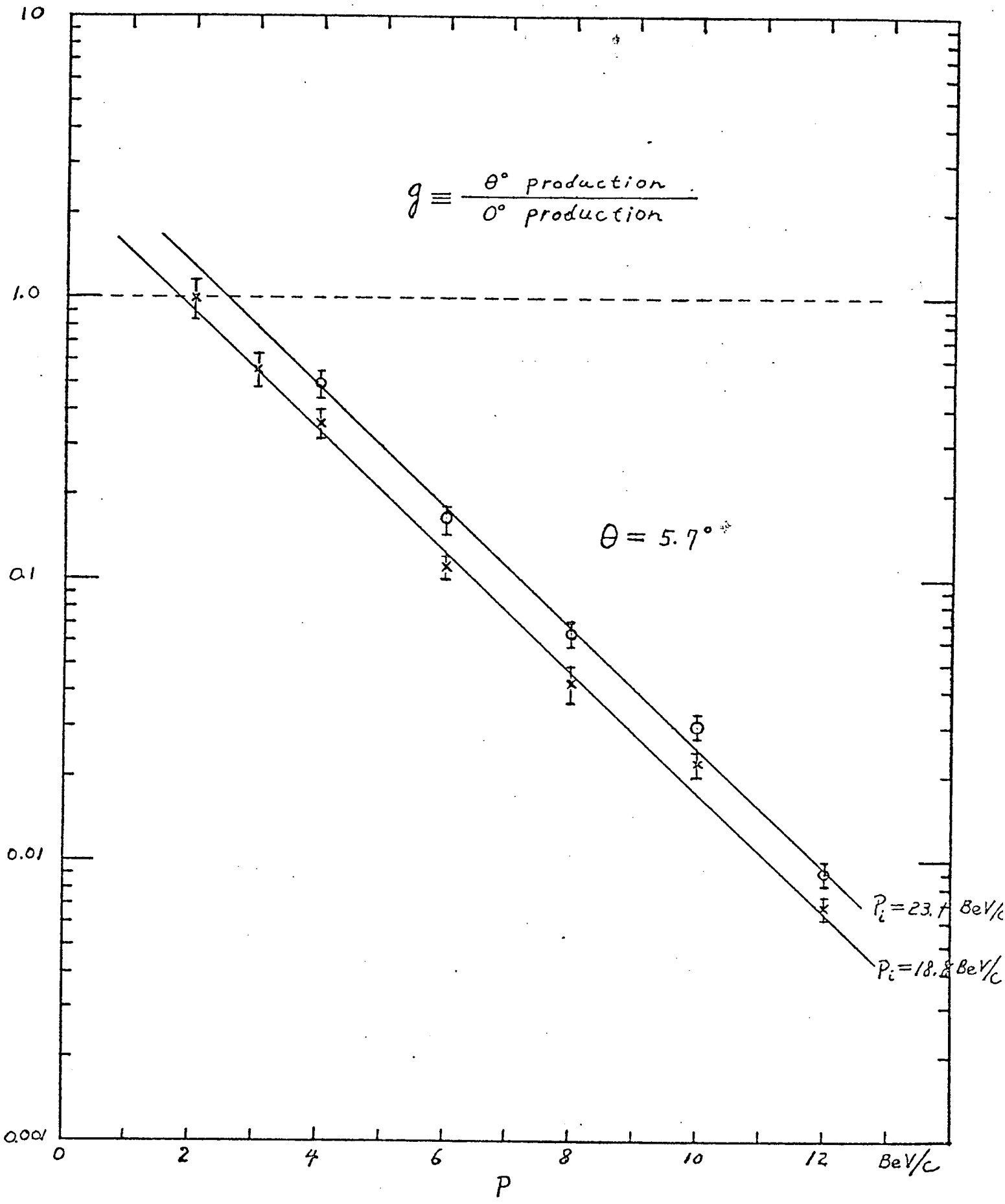
g(θ, P, Pi)
10
1.0
0.1
0.01
0.001
g ≡ θ° production / 0° production
θ = 5.7°
Pi = 23.1 BeV/c
Pi = 18.8 BeV/c
0
2
4
6
8
10
12
BeV/c
P

Fig. 1

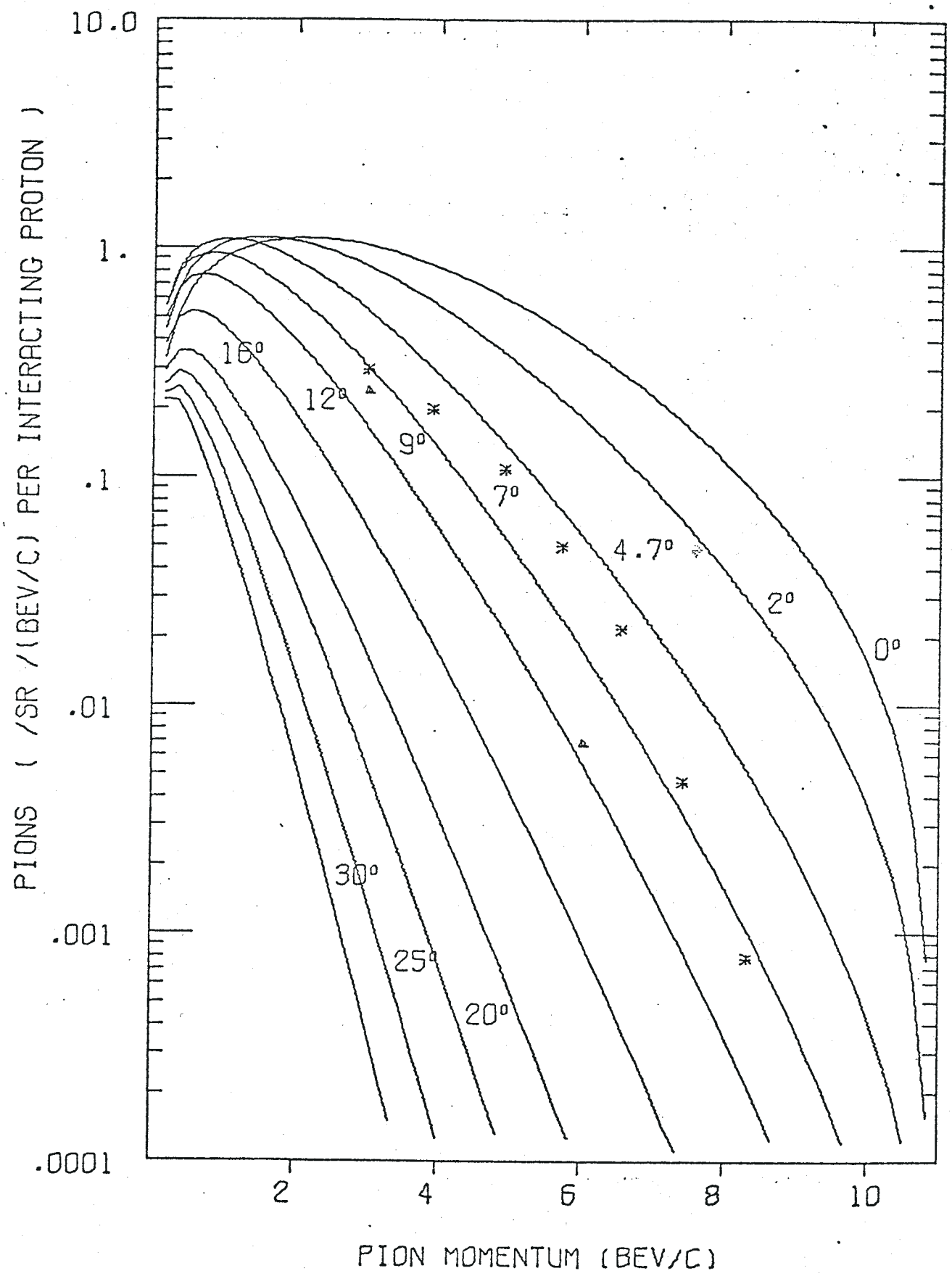
10.9 BEV/C P-BE. POSITIVE PION PRODUCTION
PIONS (/SR /(BEV/C) PER INTERACTING PROTON)
10.0
1.
.1
.01
.001
.0001
2
4
6
8
10
PION MOMENTUM (BEV/C)
16°
12°
9°
7°
4.7°
2°
0°
30°
25°
20°

Fig. 2

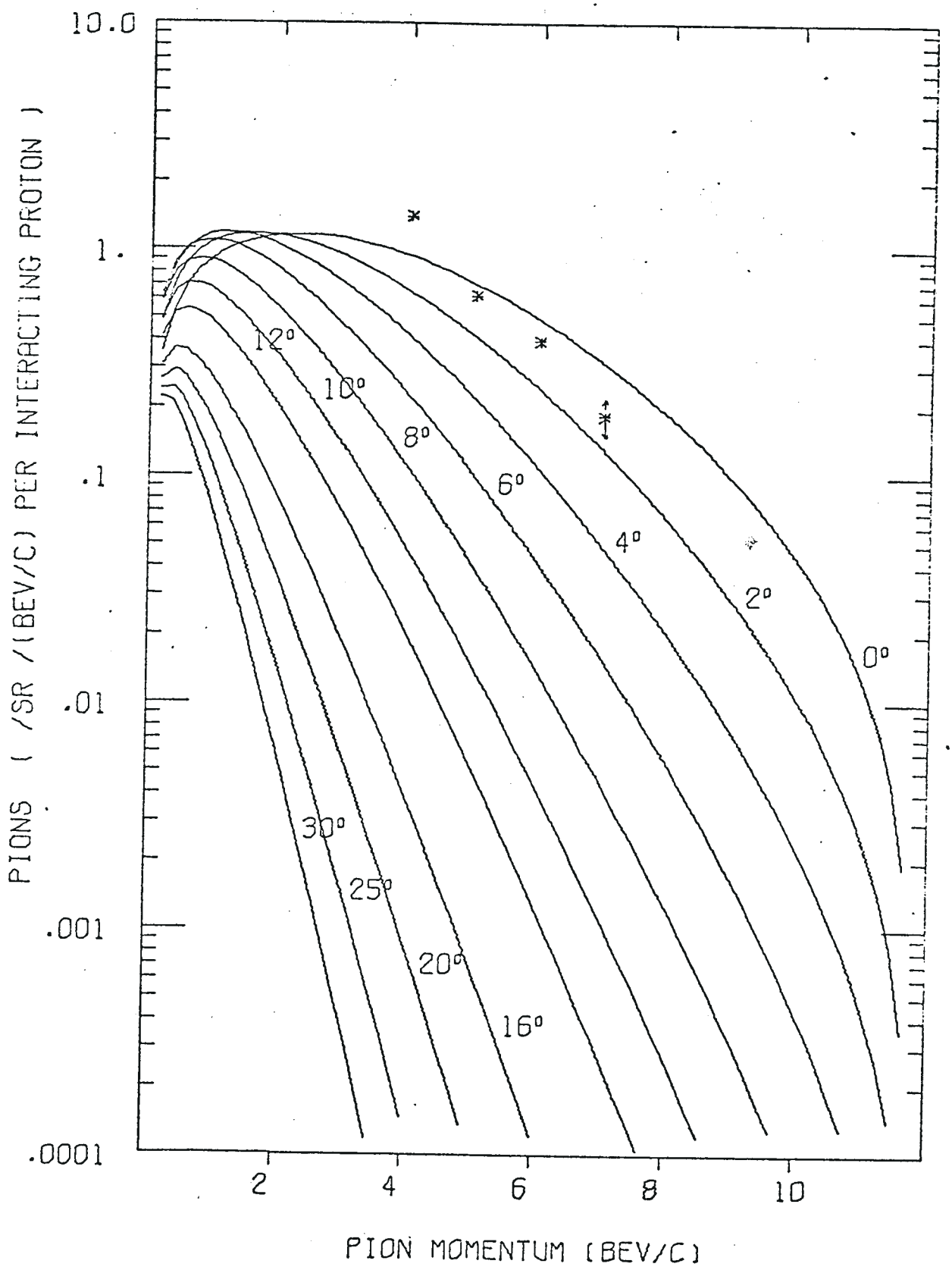
11.8 BEV/C P-BE. POSITIVE PION PRODUCTION
10.0
1.
.1
.01
.001
.0001
PIONS (/SR /(BEV/C) PER INTERACTING PROTON)
0°
2°
4°
6°
8°
10°
12°
16°
20°
25°
30°
2
4
6
8
10
PION MOMENTUM (BEV/C)

Fig. 3

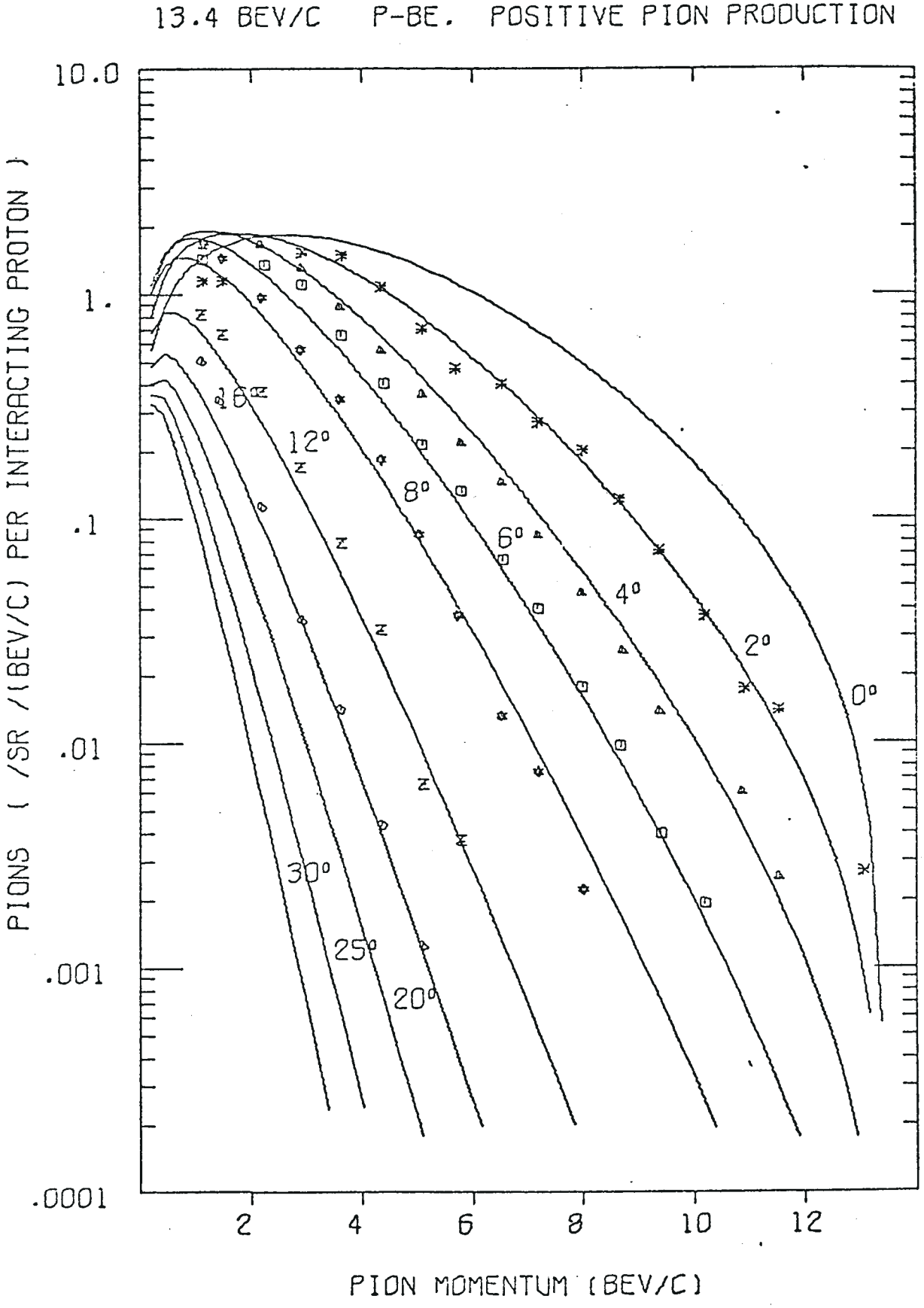
13.4 BEV/C P-BE. POSITIVE PION PRODUCTION
PIONS (/SR /(BEV/C) PER INTERACTING PROTON)
10.0
1.
.1
.01
.001
.0001
2
4
6
8
10
12
PION MOMENTUM (BEV/C)
0°
2°
4°
6°
8°
12°
16°
20°
25°
30°

Fig. 4

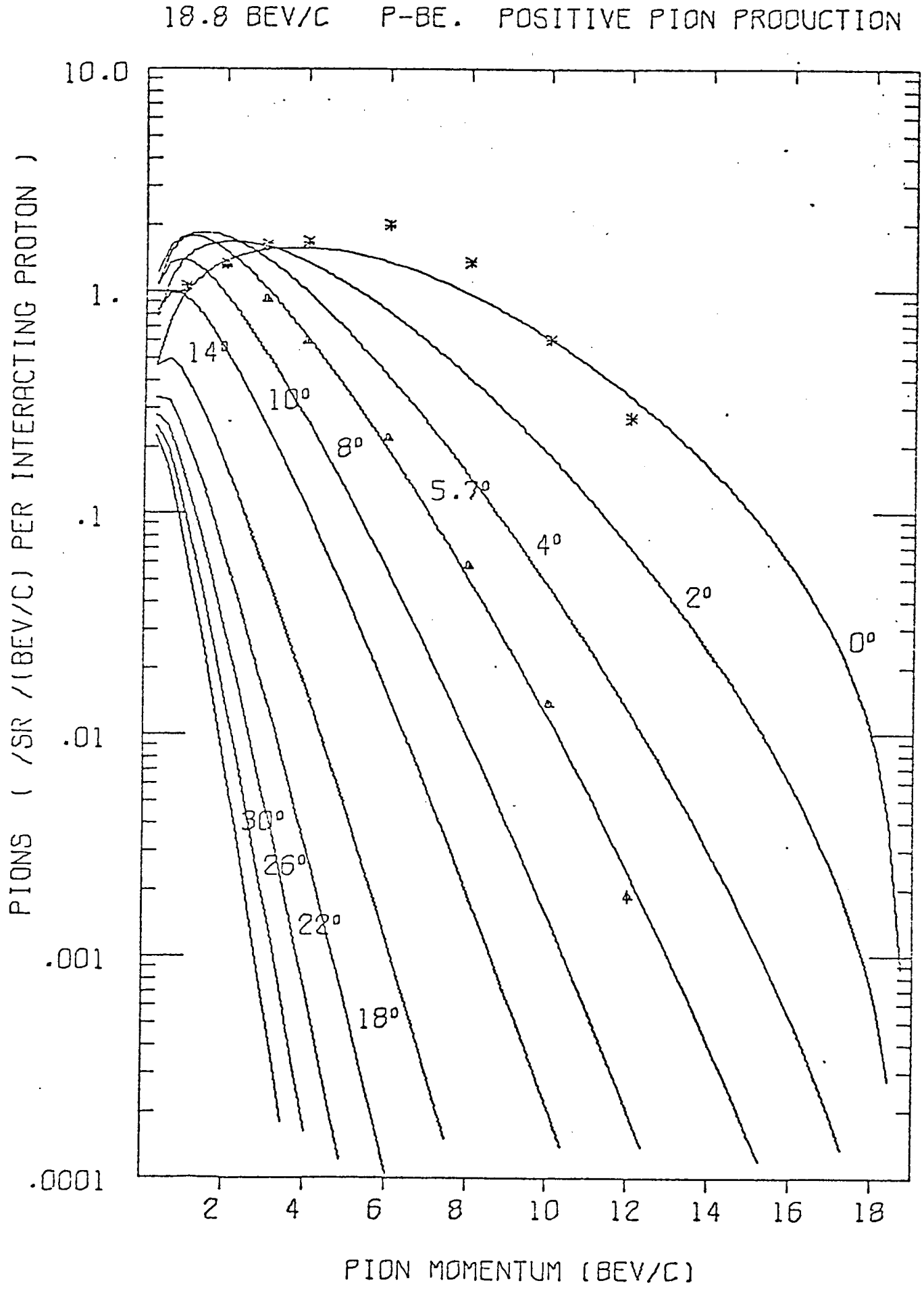
18.8 BEV/C P-BE. POSITIVE PION PRODUCTION
PIONS (/SR /(BEV/C) PER INTERACTING PROTON)
10.0
1.
.1
.01
.001
.0001
2
4
6
8
10
12
14
16
18
PION MOMENTUM (BEV/C)
0°
2°
4°
5.7°
8°
10°
14°
18°
22°
26°
30°

Fig. 5

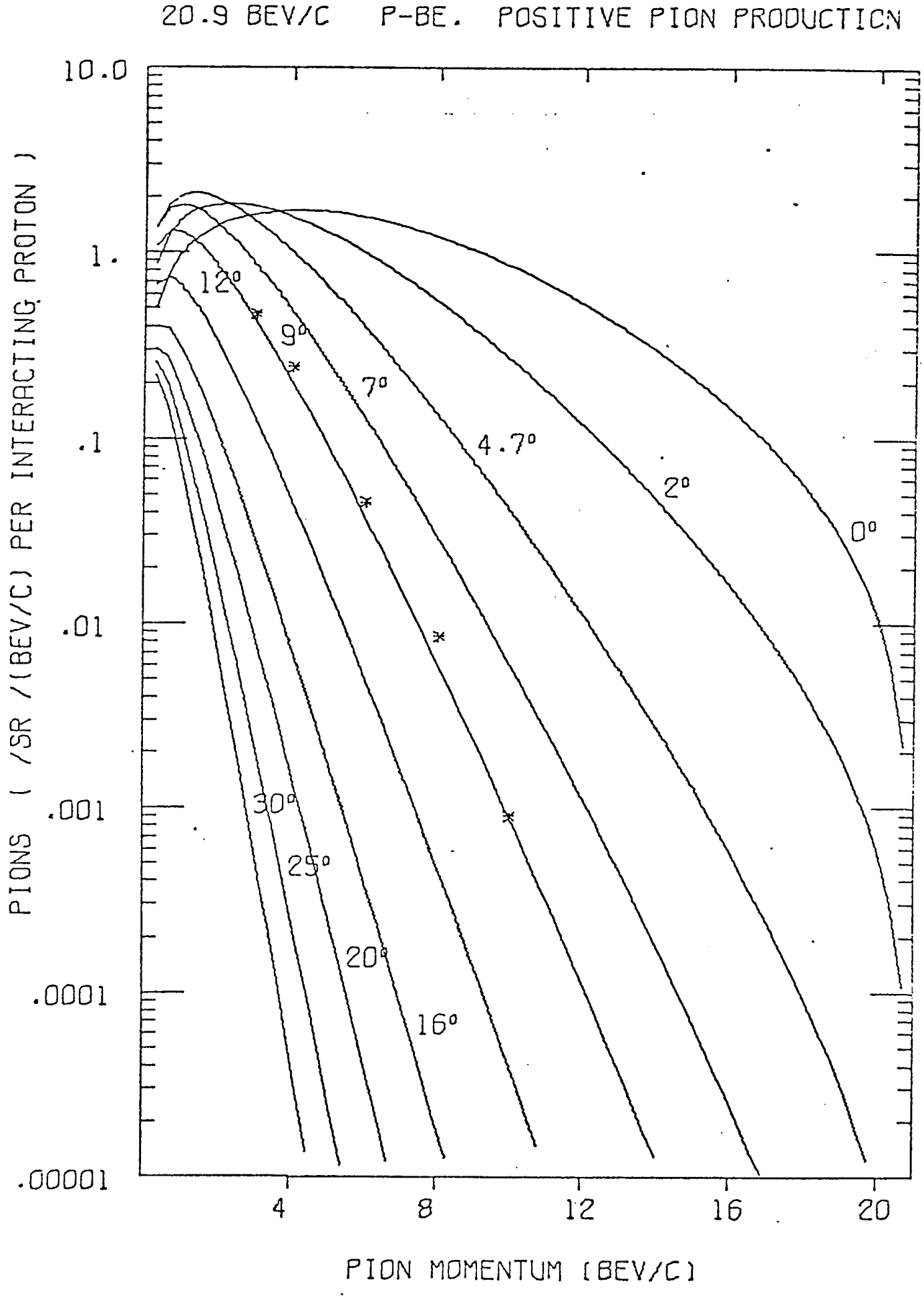
20.9 BEV/C P-BE. POSITIVE PION PRODUCTION
10.0
1.
.1
.01
.001
.0001
.00001
PIONS (/SR /(BEV/C) PER INTERACTING PROTON)
12°
9°
7°
4.7°
2°
0°
30°
25°
20°
16°
4
8
12
16
20
PION MOMENTUM (BEV/C)

Fig. 6

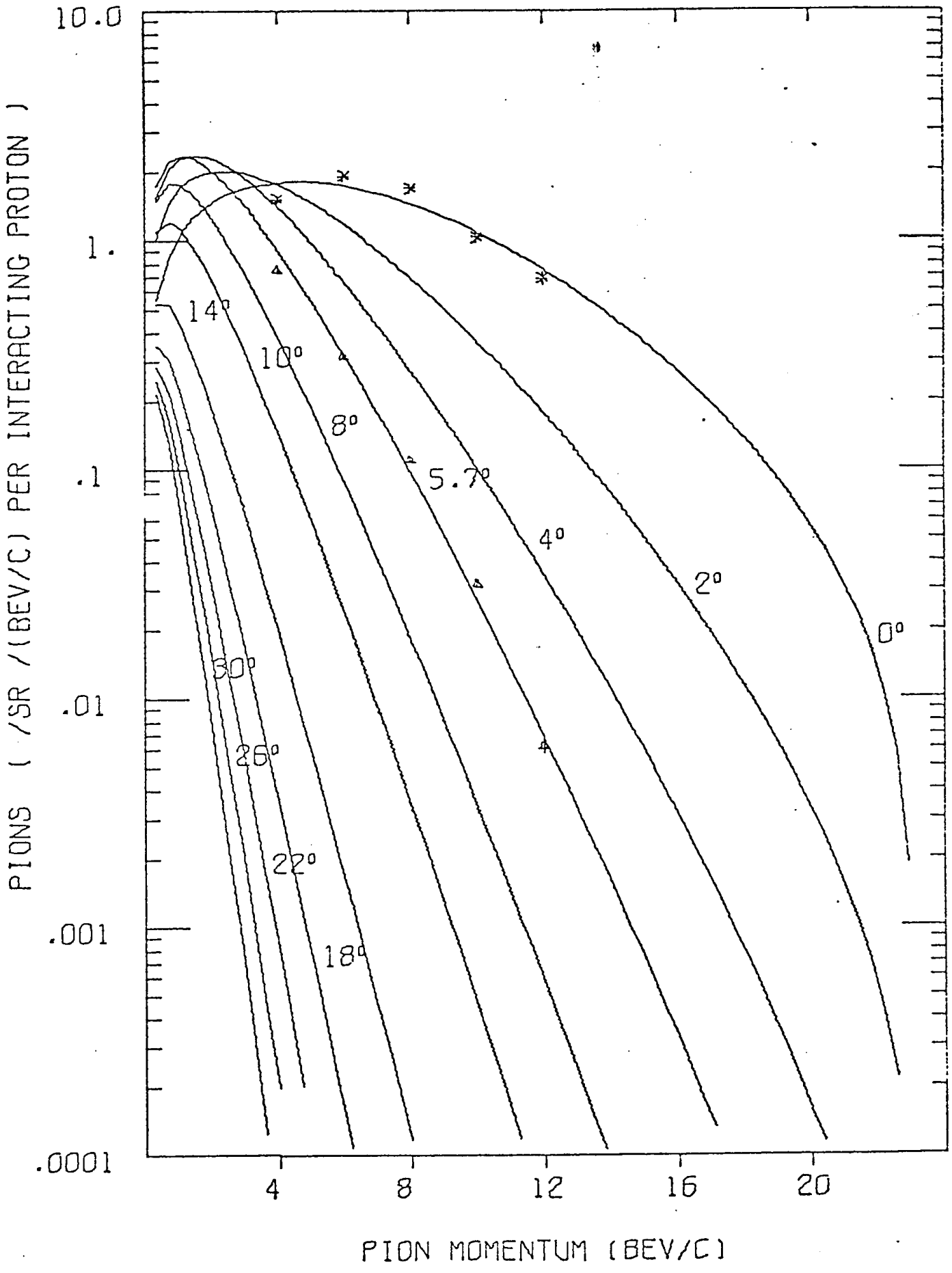
23.1 BEV/C P-BE. POSITIVE PION PRODUCTION
PIONS (/SR /(BEV/C) PER INTERACTING PROTON)
10.0
1.
.1
.01
.001
.0001
4
8
12
16
20
PION MOMENTUM (BEV/C)
0°
2°
4°
5.7°
8°
10°
14°
18°
22°
26°
30°

Fig. 7

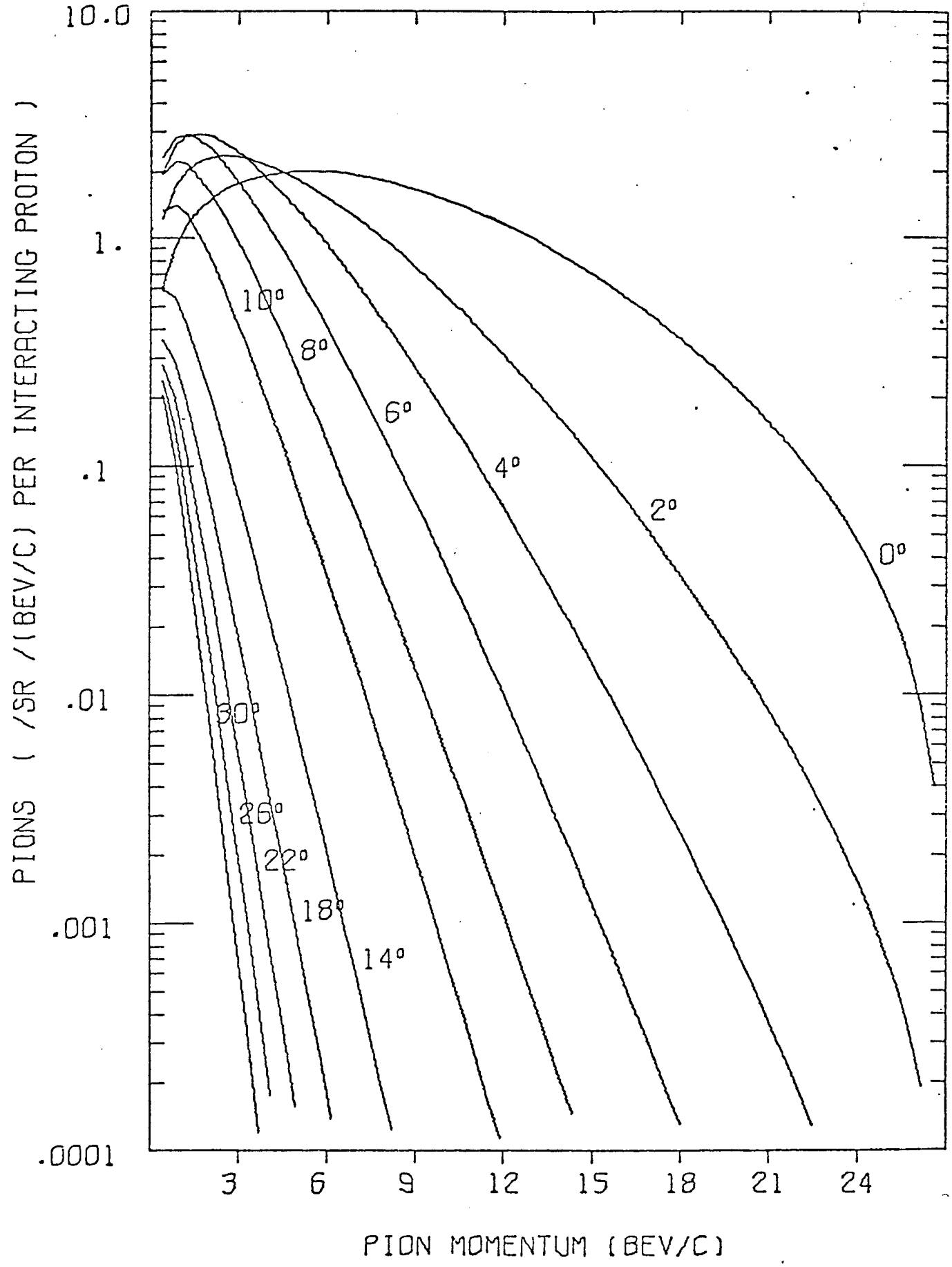
27.0 BEV/C P-BE. POSITIVE PION PRODUCTION
PIONS (/SR /(BEV/C) PER INTERACTING PROTON)
10.0
1.
.1
.01
.001
.0001
0°
2°
4°
6°
8°
10°
14°
18°
22°
26°
30°
3
6
9
12
15
18
21
24
PION MOMENTUM (BEV/C)

Fig. 8

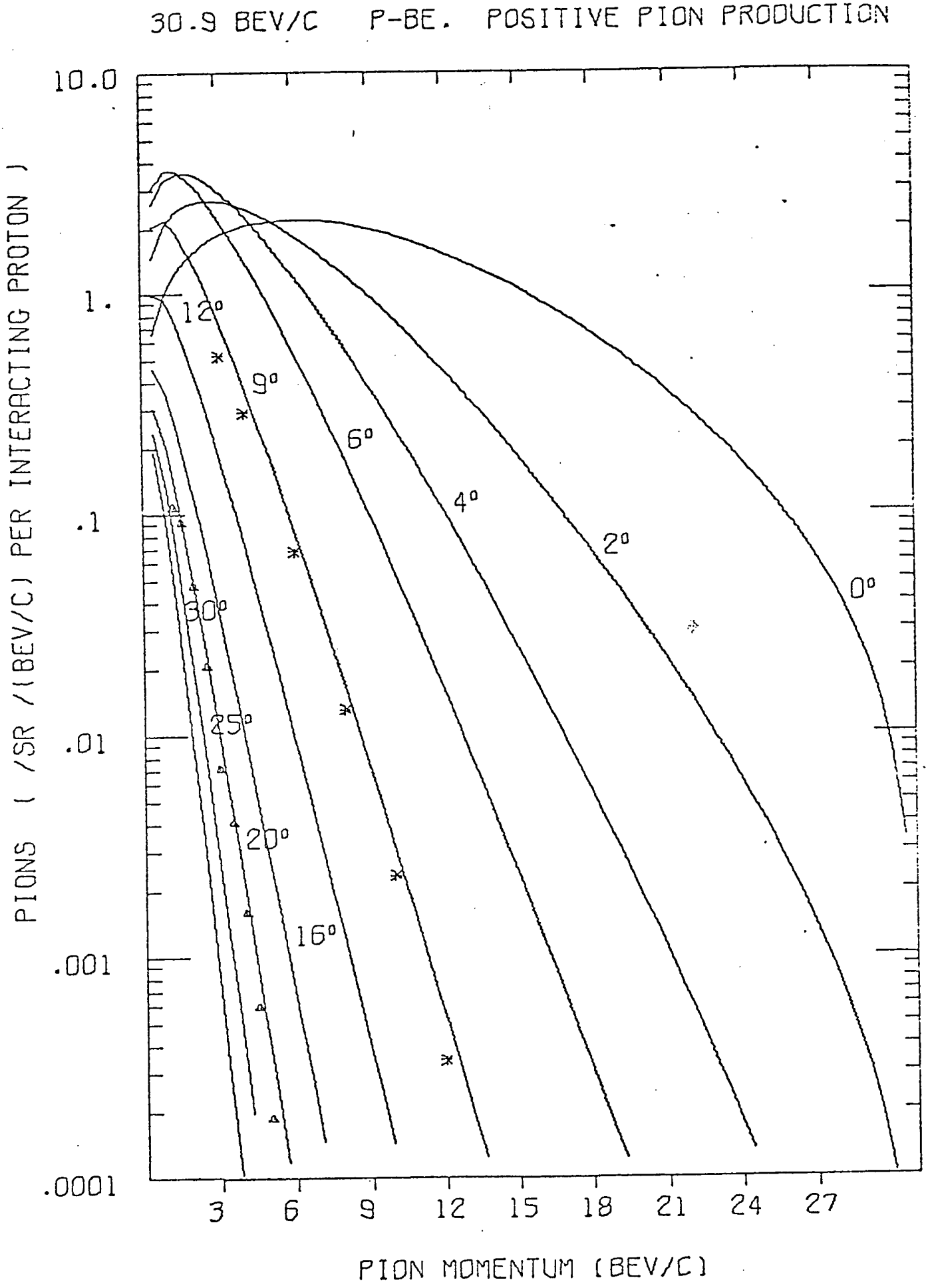
30.9 BEV/C P-BE. POSITIVE PION PRODUCTION
PIONS (/SR /(BEV/C) PER INTERACTING PROTON)
10.0
1.
.1
.01
.001
.0001
12°
9°
6°
4°
2°
0°
30°
25°
20°
16°
3
6
9
12
15
18
21
24
27
PION MOMENTUM (BEV/C)

Fig. 9

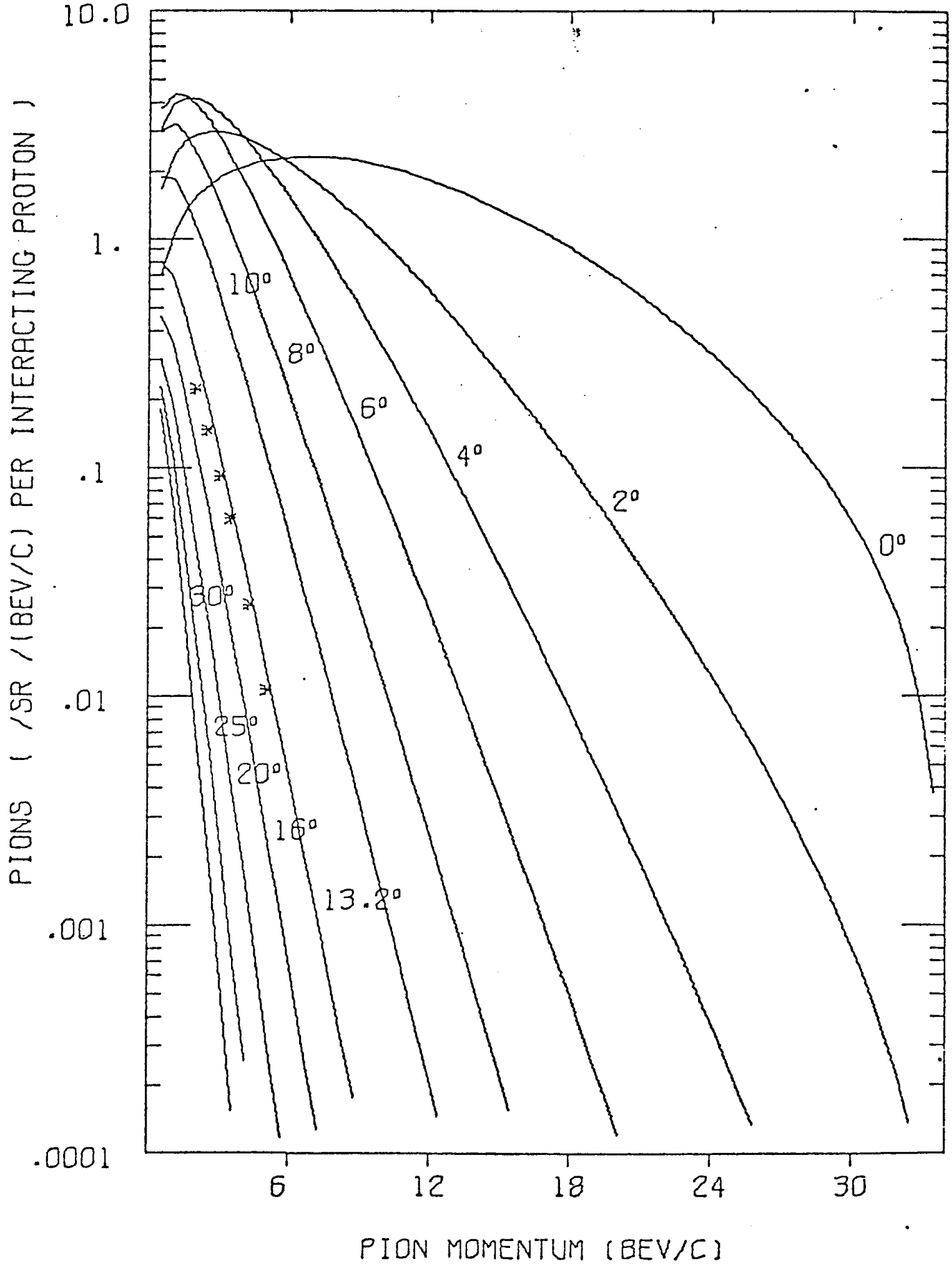
33.9 BEV/C P-BE. POSITIVE PION PRODUCTION
PIONS (/SR /(BEV/C) PER INTERACTING PROTON)
10.0
1.
.1
.01
.001
.0001
0°
2°
4°
6°
8°
10°
13.2°
16°
20°
25°
30°
6
12
18
24
30
PION MOMENTUM (BEV/C)

Fig. 10

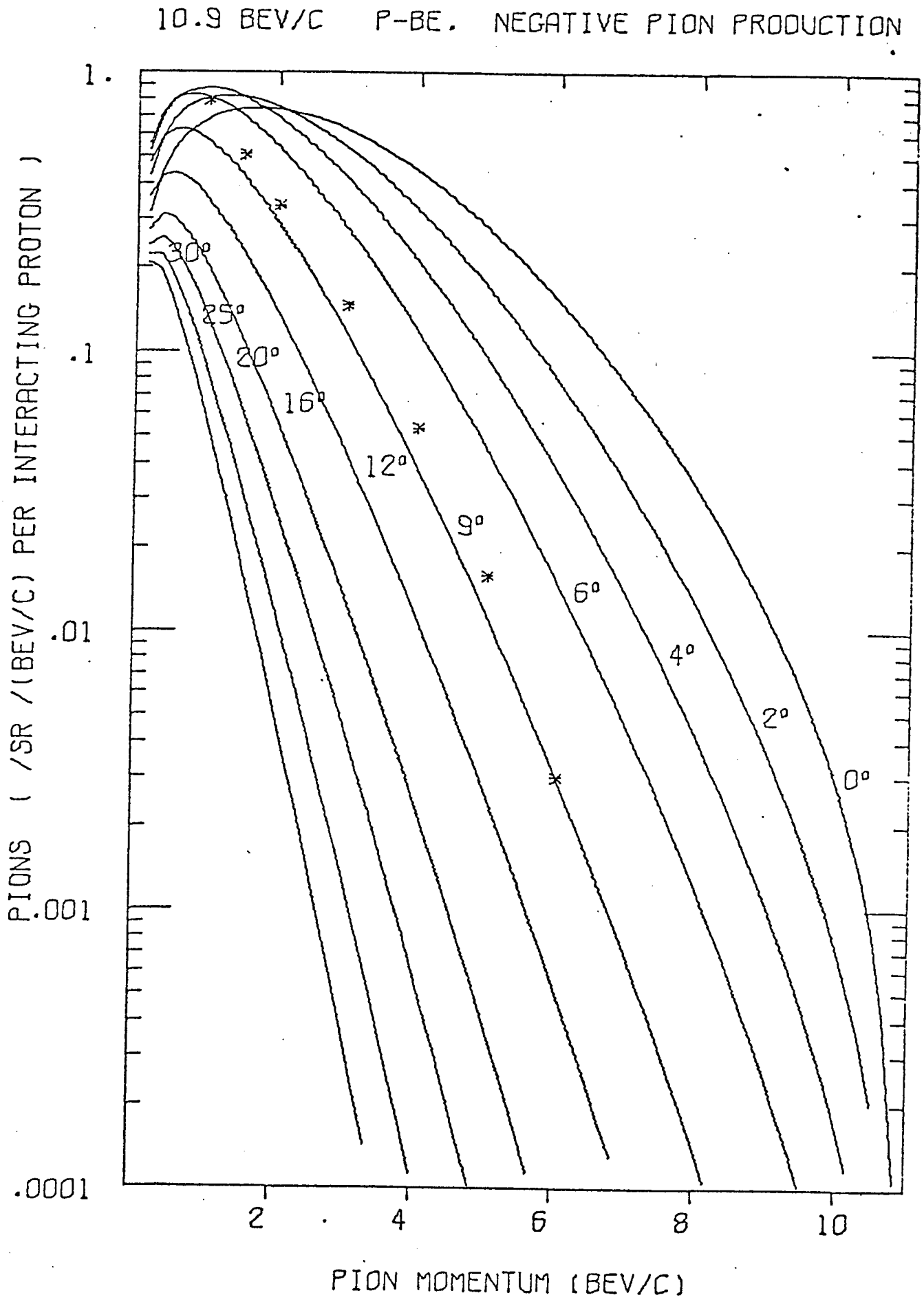
10.9 BEV/C P-BE. NEGATIVE PION PRODUCTION
PIONS (/SR /(BEV/C) PER INTERACTING PROTON)
1.
.1
.01
.001
.0001
30°
25°
20°
16°
12°
9°
6°
4°
2°
0°
2
4
6
8
10
PION MOMENTUM (BEV/C)

Fig. 11

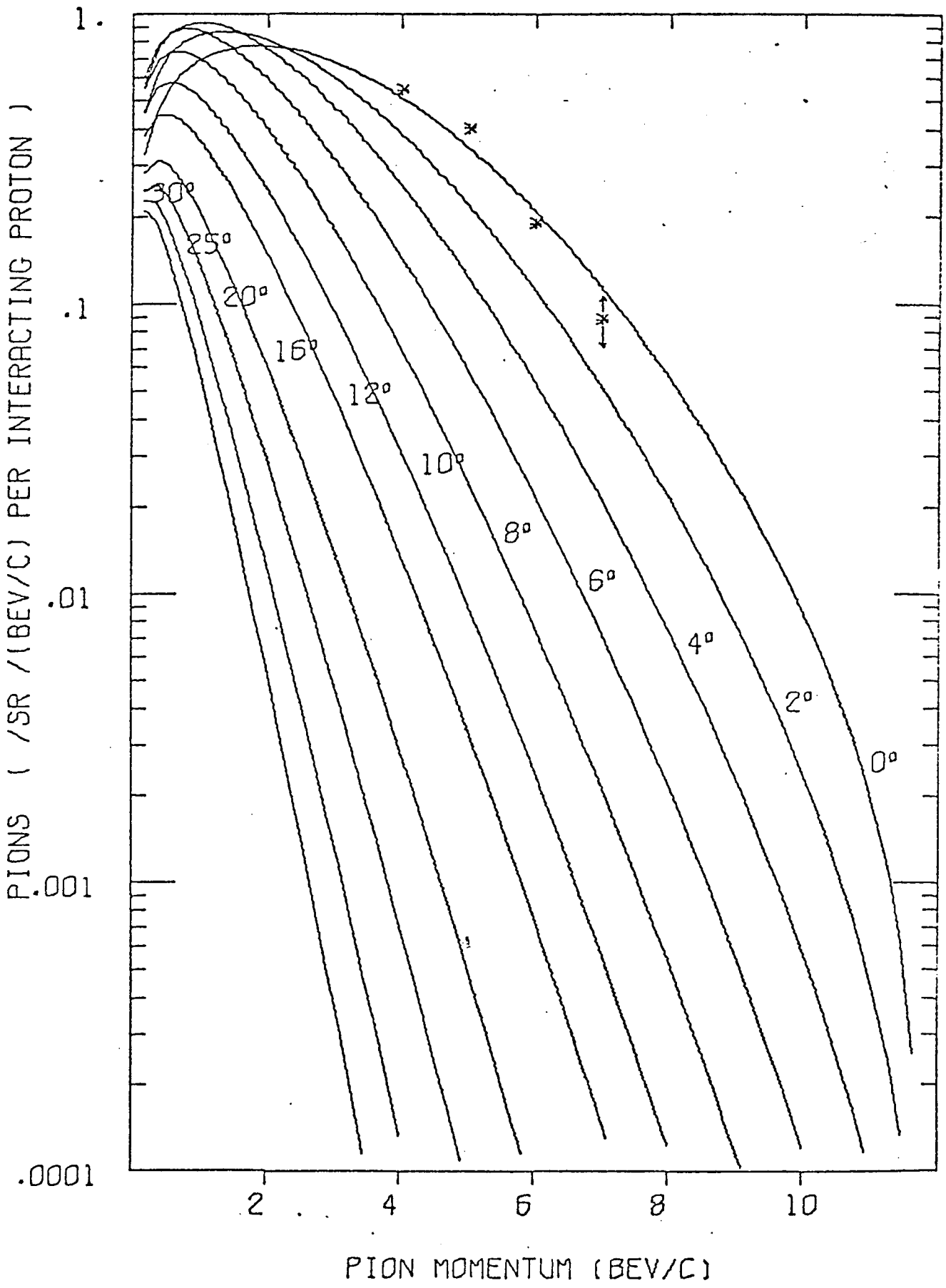
11.8 BEV/C P-BE. NEGATIVE PION PRODUCTION
PIONS (/SR /(BEV/C) PER INTERACTING PROTON)
1.
.1
.01
.001
.0001
30°
25°
20°
16°
12°
10°
8°
6°
4°
2°
0°
2
4
6
8
10
PION MOMENTUM (BEV/C)

Fig. 12

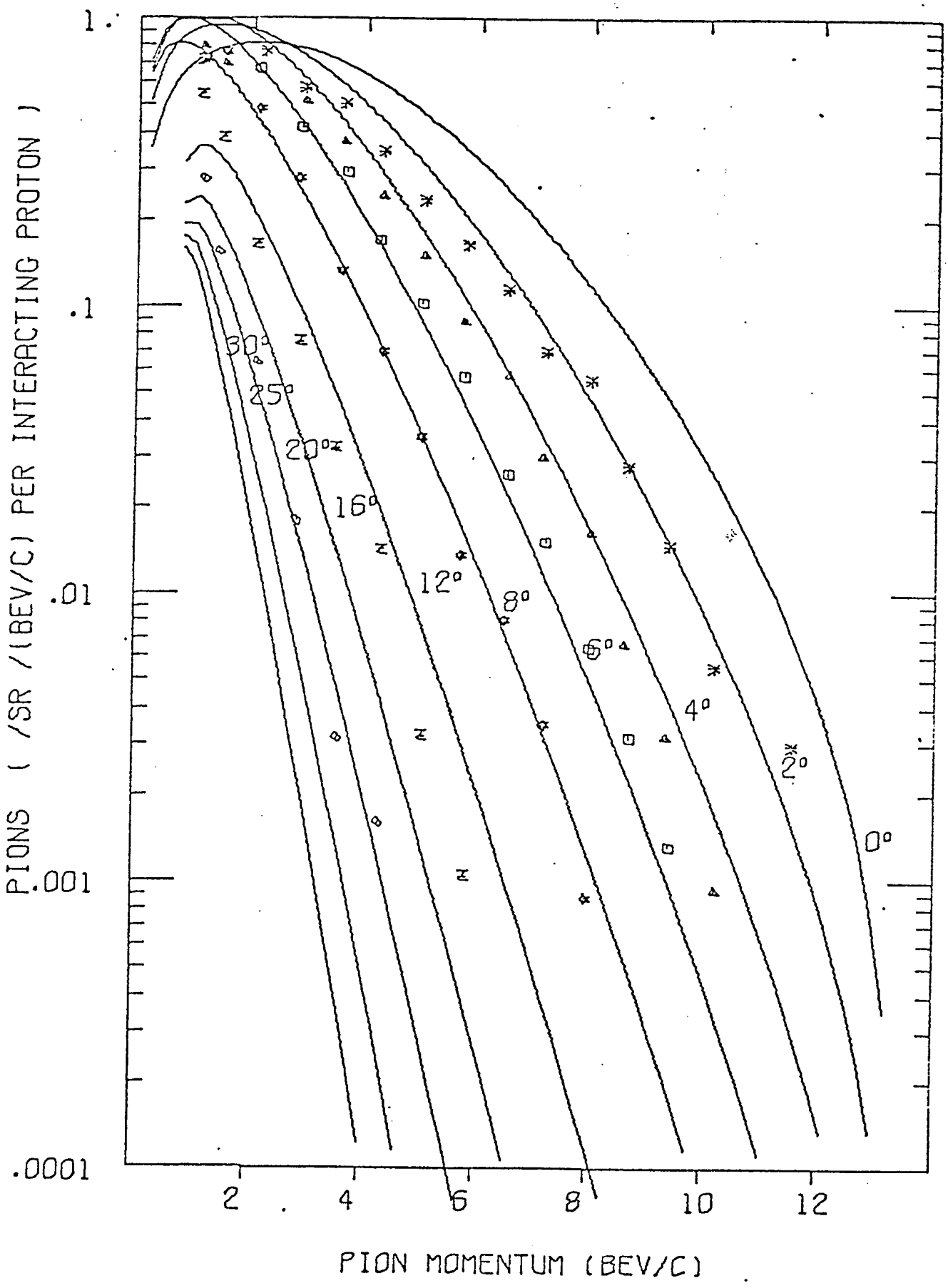
13.4 BEV/C P-BE. NEGATIVE PION PRODUCTION
PIONS (/SR /(BEV/C) PER INTERACTING PROTON)
1.
.1
.01
.001
.0001
2
4
6
8
10
12
PION MOMENTUM (BEV/C)
0°
2°
4°
6°
8°
12°
16°
20°
25°
30°

Fig. 13

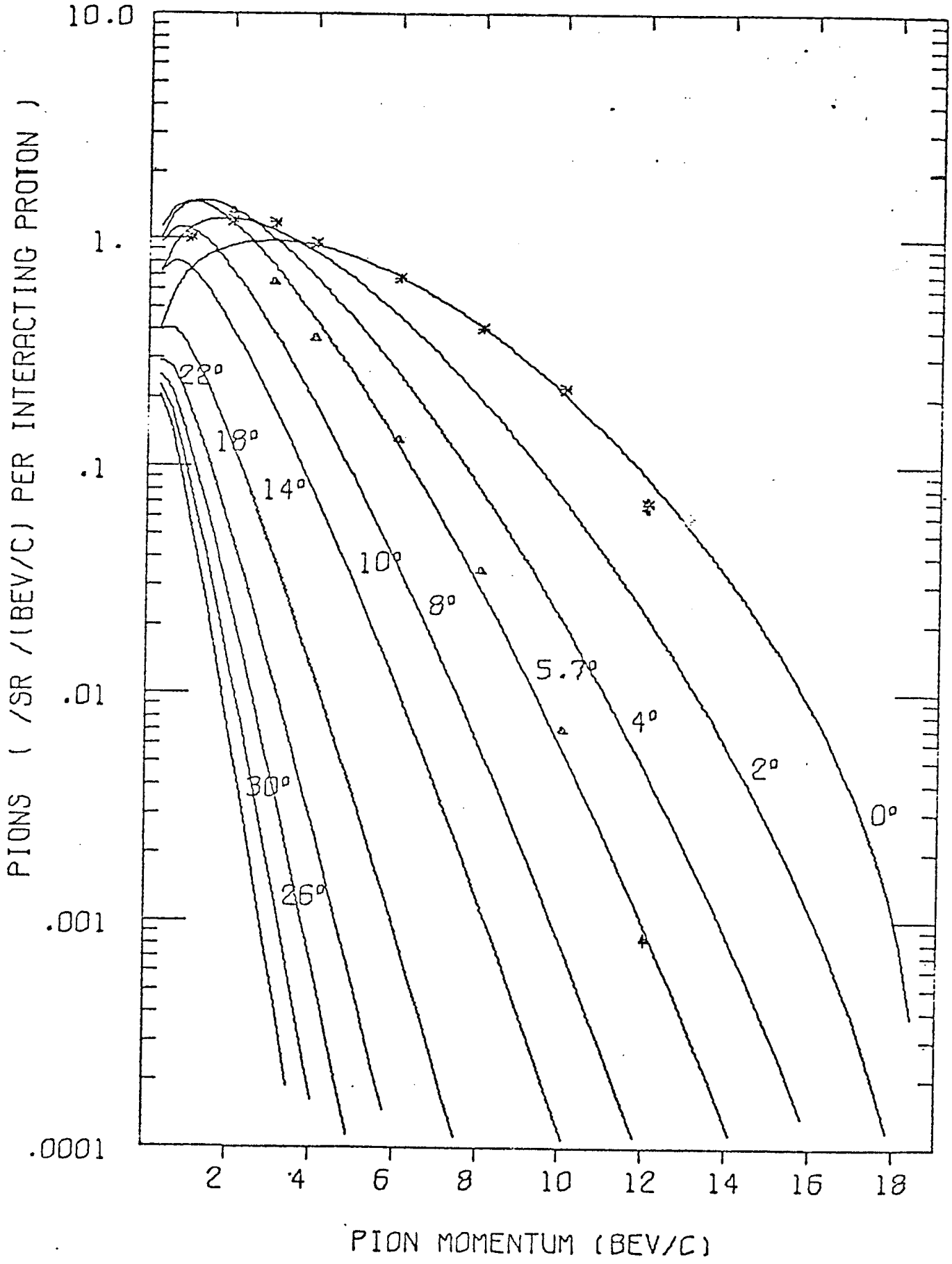
18.8 BEV/C P-BE. NEGATIVE PION PRODUCTION
PIONS (/SR /(BEV/C) PER INTERACTING PROTON)
10.0
1.
.1
.01
.001
.0001
22°
18°
14°
10°
8°
5.7°
4°
2°
0°
30°
26°
2
4
6
8
10
12
14
16
18
PION MOMENTUM (BEV/C)

Fig. 14

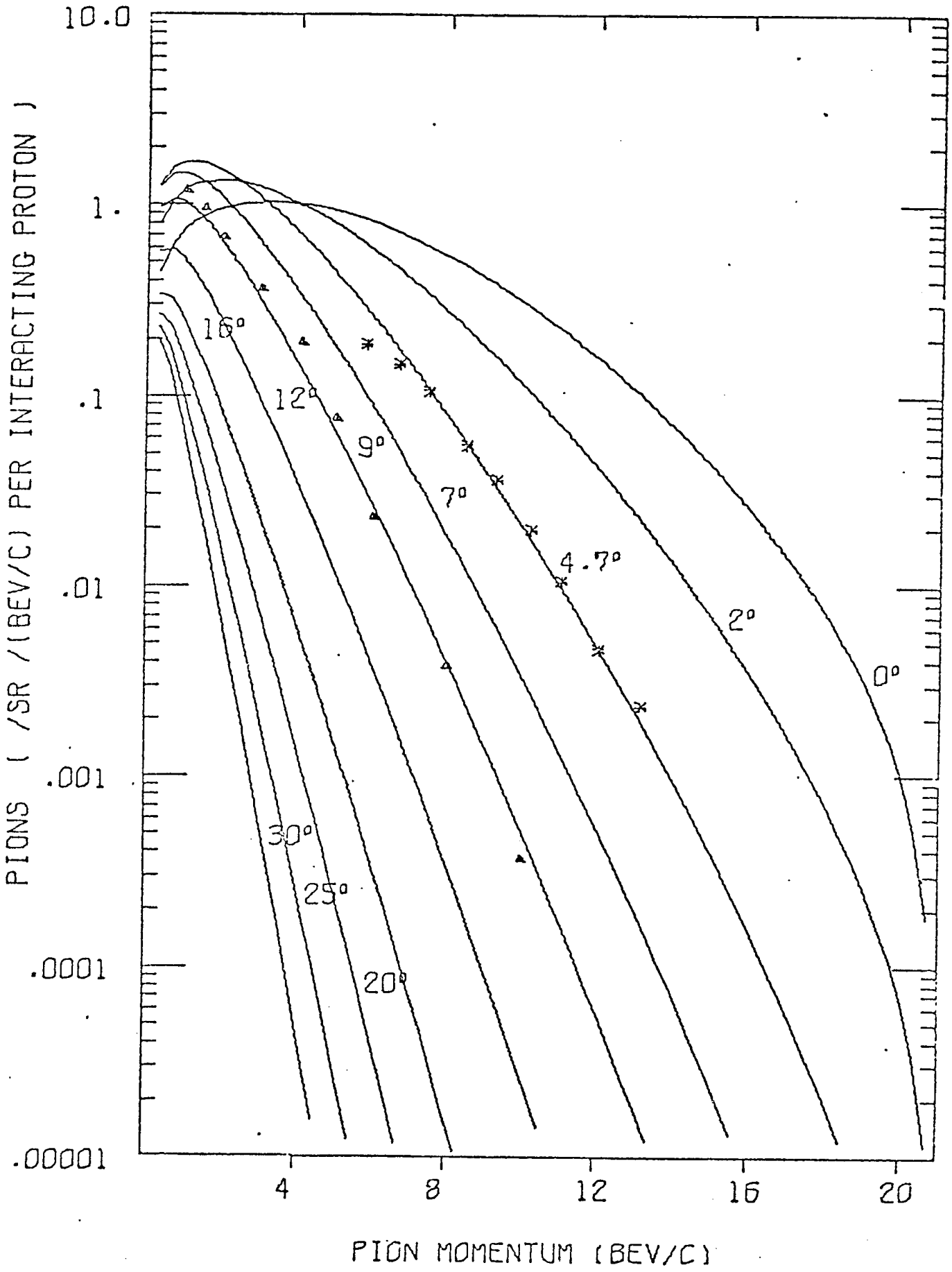
20.9 BEV/C P-BE. NEGATIVE PION PRODUCTION
PIONS (/SR /(BEV/C) PER INTERACTING PROTON)
10.0
1.
.1
.01
.001
.0001
.00001
16°
12°
9°
7°
4.7°
2°
0°
30°
25°
20°
4
8
12
16
20
PION MOMENTUM (BEV/C)

Fig. 15

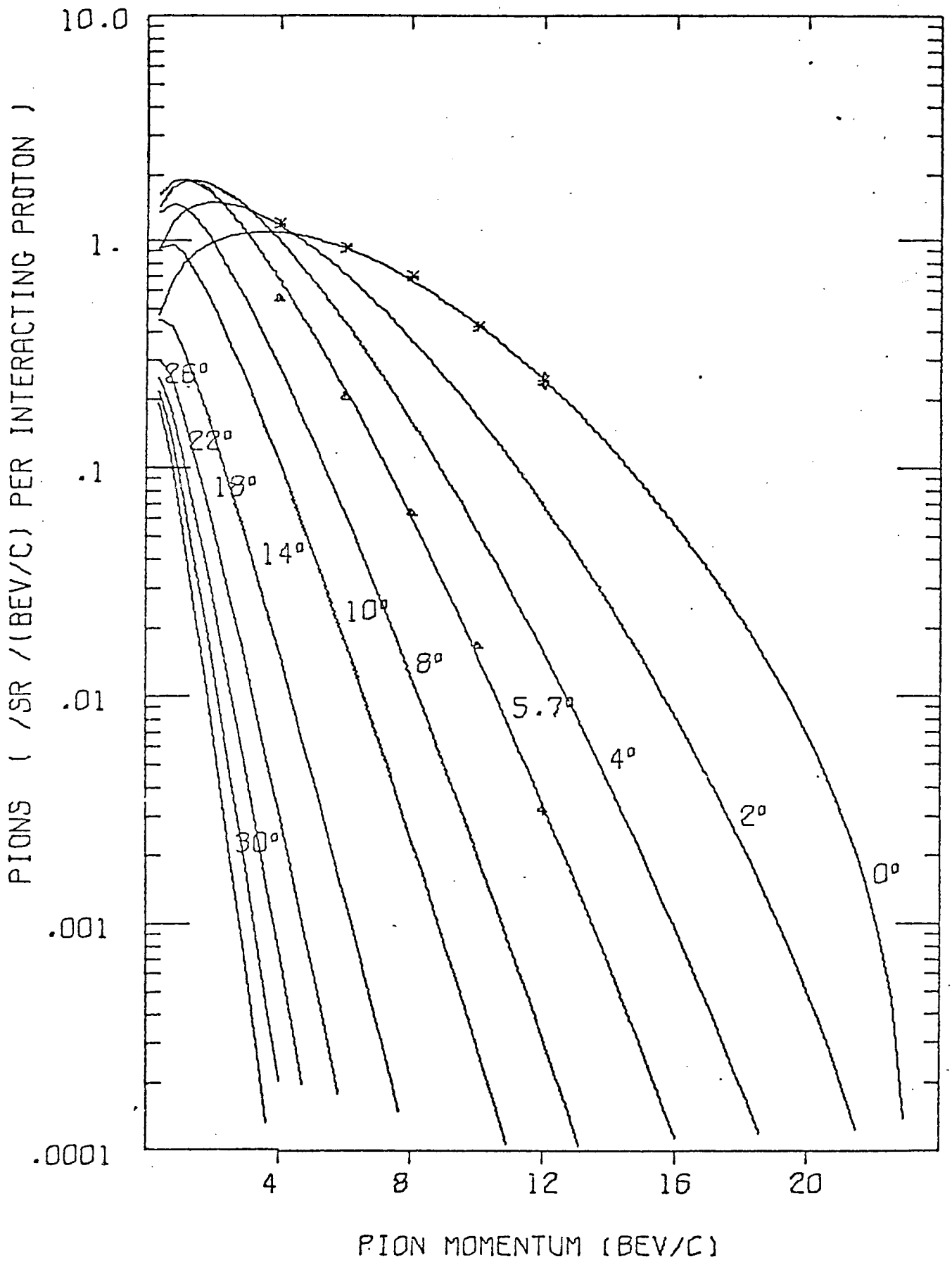
23.1 BEV/C P-BE. NEGATIVE PION PRODUCTION
PIONS (/SR /(BEV/C) PER INTERACTING PROTON)
10.0
1.
.1
.01
.001
.0001
4
8
12
16
20
PION MOMENTUM (BEV/C)
26°
22°
18°
14°
10°
8°
5.7°
4°
2°
0°
30°

Fig. 16

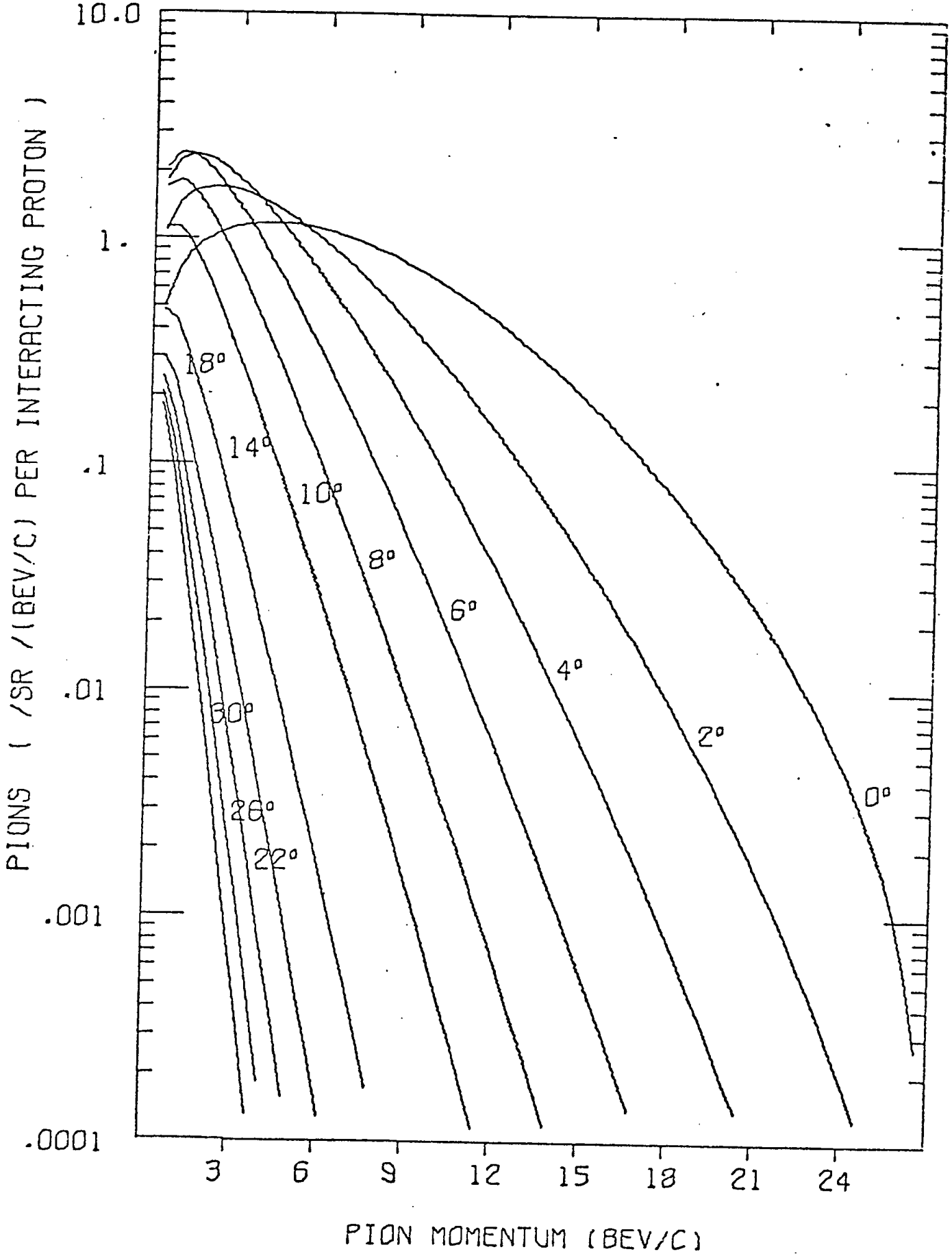
27.0 BEV/C P-BE. NEGATIVE PION PRODUCTION
PIONS (/SR /(BEV/C) PER INTERACTING PROTON)
10.0
1.
.1
.01
.001
.0001
3
6
9
12
15
18
21
24
PION MOMENTUM (BEV/C)
0°
2°
4°
6°
8°
10°
14°
18°
22°
26°
30°

Fig. 17

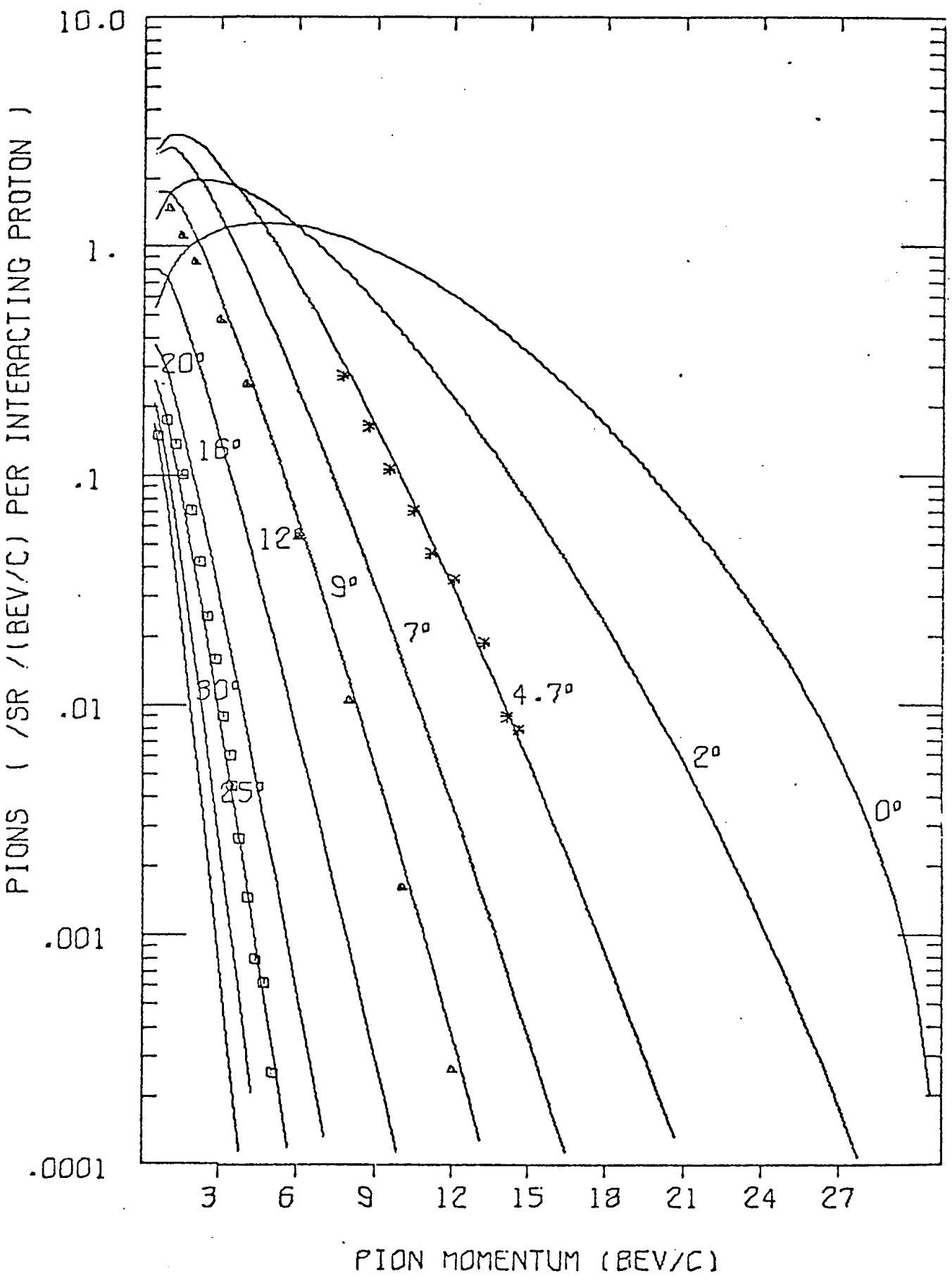
30.9 BEV/C P-BE. NEGATIVE PION PRODUCTION
PIONS (/SR /(BEV/C) PER INTERACTING PROTON)
10.0
1.
.1
.01
.001
.0001
20°
16°
12°
9°
7°
4.7°
2°
0°
30°
25°
3
6
9
12
15
18
21
24
27
PION MOMENTUM (BEV/C)

Fig. 18

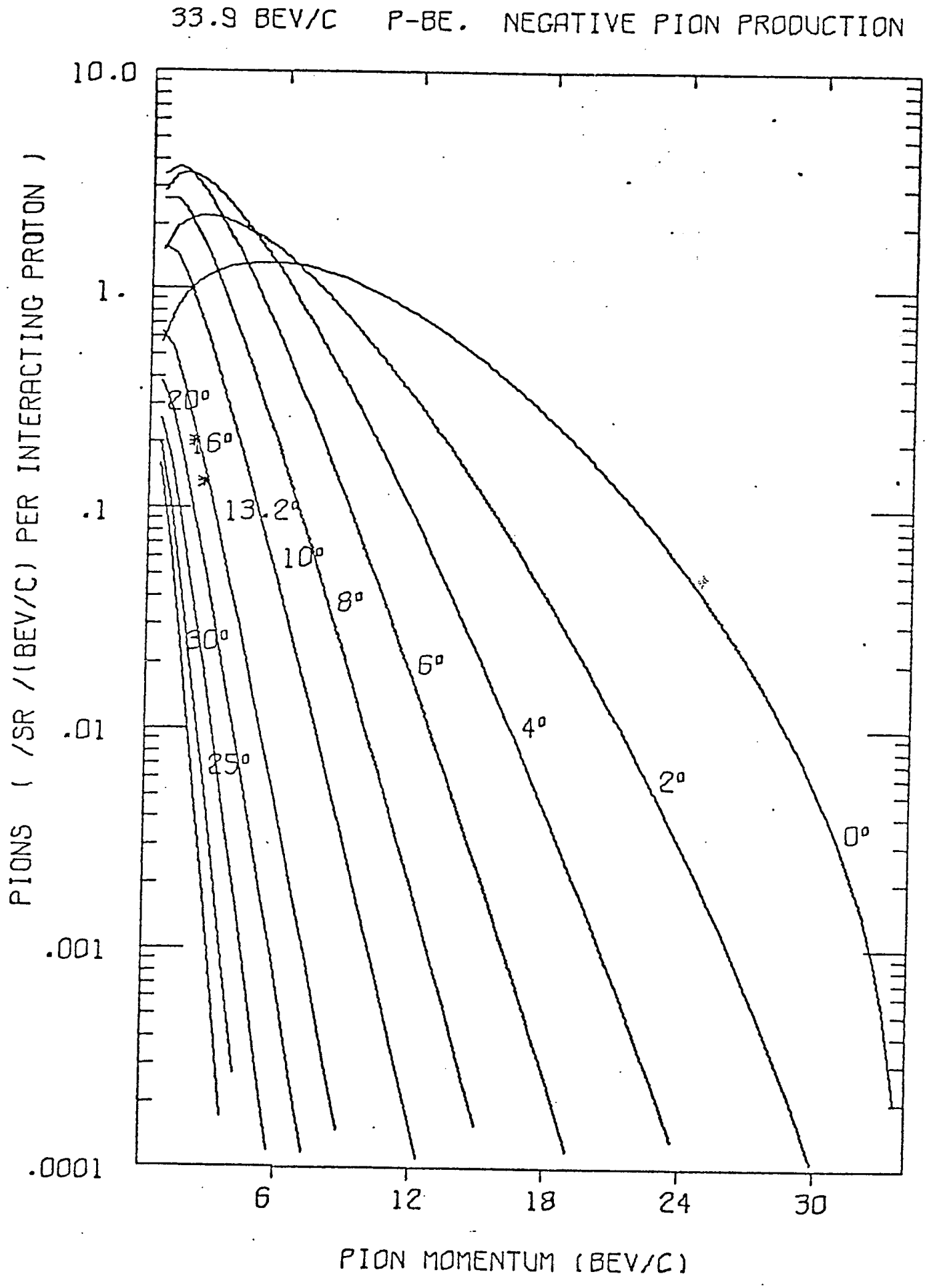
33.9 BEV/C P-BE. NEGATIVE PION PRODUCTION
PIONS (/SR /(BEV/C) PER INTERACTING PROTON)
10.0
1.
.1
.01
.001
.0001
0°
2°
4°
6°
8°
10°
13.2°
16°
20°
25°
30°
6
12
18
24
30
PION MOMENTUM (BEV/C)

Fig. 19

References

1. D. Dekkers, J.A. Geibel, R. Mermod, G. Weber, T.R. Willitts, K. Winter, B. Jordan, M. Vivargent, N.M. King and E.J.N. Wilson, Physical Review, 137, B962 (1965).

2. R.A. Lundy, T.B. Novey, D.D. Yavanovitch and V.L. Telegdi, Physical Review Letters, 14, 504 (1966).

3. W.F. Baker, R.L. Cool, W.E. Jenkins, T.F. Kycia, S.J. Lindenbaum, W.A. Love, D. Luers, J.A. Niederer, S. Ozaki, A.L. Read, J.J. Russell and L.C.L. Yuan, Physical Review Letters 7, 101 (1961).

4. V.L. Fitch, S.L. Meyer and P.A. Pirone, Physical Review 126, 1849 (1962).

5. G. Belletlini, G. Cocconi, A.N. Diddens, E. Lillethan, G. Matthiae, J.P. Scanlon and A.M. Wetherall, CERN Report PS/5037/KL, (1965). (Unpublished).

6. F. Ragusa, "Modified Version of Los Alamos Code "PAKAG."" (In file at the BNL Program Library)

7. G. von Dardel, CERN/NP, Internal Report 62-17, 1962. (Unpublished).

8. R. Burns, K. Goulianos, E. Hyman, L. Lederman, W. Lee, N. Mistry, J. Rettberg, M. Schwartz, J. Steinberger and J. Sunderland, "Informal Conference on Experimental Neutrino Physics," p.97 CERN 65-32, 1965. (Unpublished).

9. J. Ranft, CERN/MPS, Internal Report MU/EP 66-4, 1966. (Unpublished). This work influenced our functional form of the forward production.

10. G. Cocconi, L.J. Koester and D.H. Perkins, "The Berkeley High Energy Physics Study," UCRL-10022, p.167, 1961. (Unpublished).

11. P. Haberler, CERN/MPS, Internal Report, DL 63-23/Rev. 1, 1963. (Unpublished).

12. G. Trilling, Lawrence Radiation Laboratory, Internal Report UCID-10148, 1966. (Unpublished).

Figure Captions

Fig. 1 Function g for $\theta = 5.7^{\circ}$ and incident proton momenta 18.8 and 23.1 BeV/c. g is the ratio of θ° production to 0° production. The data are derived from the data of Reference 1. The straight lines are simple eye-ball fits to the data.

Fig. 2 Momentum spectra for π^+ production from P-Be collision at 10.9 BeV/c incident momentum. The data are from Reference 3.

Fig. 3 Momentum spectra for π^+ production from P-Be collision at 11.8 BeV/c incident momentum. The data are from Reference 1.

Fig. 4 Momentum spectra for π^+ production from P-Be collision at 13.4 BeV/c incident momentum. The data are from Reference 2.

Fig. 5 Momentum spectra for π^+ production from P-Be collision at 18.8 BeV/c incident momentum. The data are from Reference 1.

Fig. 6 Momentum spectra for π^+ production from P-Be collision at 20.9 BeV/c incident momentum. The data are from Reference 3.

Fig. 7 Momentum spectra for π^+ production from P-Be collision at 23.1 BeV/c incident momentum. The data are from Reference 1.

Fig. 8 Momentum spectra for π^+ production from P-Be collision at 27.0 BeV/c incident momentum.

Fig. 9 Momentum spectra for π^+ production from P-Be collision at 30.9 BeV/c incident momentum. The data are from Reference 3.

Fig. 10 Momentum spectra for π^+ production from P-Be collision at 33.9 BeV/c incident momentum. The data are from Reference 4.

Fig. 11 Momentum spectra for π^- production from P-Be collision at 10.9 BeV/c incident momentum. The data are from Reference 3.

Fig. 12 Momentum spectra for π^- production from P-Be collision at 11.8 BeV/c incident momentum. The data are from Reference 1.

Fig. 13 Momentum spectra for π^- production from P-Be collision at 13.4 BeV/c incident momentum. The data are from Reference 2.

Fig. 14 Momentum spectra for π^- production from P-Be collision at 18.8 BeV/c incident momentum. The data are from Reference 1.

Fig. 15 Momentum spectra for π^- production from P-Be collision at 20.9 BeV/c incident momentum. The data are from Reference 3.

Fig. 16 Momentum spectra for π^- production from P-Be collision at 23.1 BeV/c incident momentum. The data are from Reference 1.

Figure Captions

Fig. 17 Momentum spectra for π^- production from P-Be collision at 27.0 BeV/c incident momentum.

Fig. 18 Momentum spectra for π^- production from P-Be collision at 30.9 BeV/c incident momentum. The data are from Reference 3.

Fig. 19 Momentum spectra for π^- production from P-Be collision at 33.9 BeV/c incident momentum. The data are from Reference 4.

study of the behavior of g at 13.4 BeV/c supports the observation at 18.8 and 23.1 BeV/c; namely, the slope h is independent of the incident momentum P_i, and is a function of the production angle θ alone. Assuming this to be true at 30 BeV, we thus obtain an expression

$$g = e^{-h(\theta)\ (P-P_c)} \qquad (1)$$

Now h has to vanish at $\theta = 0$, where g reduces to 1. Furthermore, the data at 13.4 BeV/c indicate that P_c decreases as θ increases, while the data at 18.8 and 23.1 BeV/c show that P_c increases as the incident momentum increases. To accommodate these features we chose the functional forms

$$h = a\ \theta^m \qquad (2)$$

$$P_c = b\ P_i\ \cos^n\theta \qquad (3)$$

where a, b, m, and n are unknown constants to be determined by the least square analysis.

2. Forward Production

The general characteristics of the forward production as observed on the semi-log plot are:

1. The momentum spectrum decays with a power greater than one.
2. The higher the incident momentum, the slower the decay of the momentum spectrum, and
3. The momentum spectrum has a maximum and decreases rapidly as the secondary momentum approaches zero.

In addition to these characteristics, the momentum spectrum has to satisfy a certain kinematical requirement, namely

4. The spectrum must vanish as the secondary momentum reaches the incident momentum, (slightly below the incident momentum, to be exact). To satisfy above features, we assume for the forward production spectrum the functional form

$$f = C_1 P^{C_2} \left(1 - \frac{P}{P_i}\right) e^{-\frac{C_3 P^{C_4}}{P_i^{C_5}}} \qquad (4)$$

where C_1 through C_5 are unknown constants to be determined.

3. Least Square Analysis

Combining the forward production f and the angular dependent term g, we have the complete double differential momentum spectrum

$$\frac{d^2N}{d\Omega dp} = f.g$$

$$= C_1 P^{C_2} \left(1 - \frac{P}{P_i}\right) e^{-\frac{C_3 P^{C_4}}{P^{C_6}}} - C_6 \theta^m \left(P - C_7 P_i \cos^{C_8} \theta\right) \qquad (5)$$

where C_1 through C_8 and m are the parameters to be determined by the least square fitting to the experimental data (m turned out to be 1). The data used in the analysis are from four experiments; by Lundy et al., at 13.4 BeV/c[2], Dekkers et al., at 11.8, 18.8 and 23.1 BeV/c[1]; Baker et al., at 10.9, 20.9 and 30.9 BeV/c[3] and Fitch et al., at 33.9 BeV/c[4].

A. Normalization of the Experimental Data

In view of the relatively limited experimental data, every bit of them is of great value. The data of Lundy et al. cover most thoroughly the detailed angular dependence of the momentum spectrum, and are thus invaluable in determining the function h (θ), while the data of Dekkers et al. are the sole data which present the forward productions and are particularly useful in determining the function f. The data of Baker et al. on the other hand, covered the largest range of the incident momentum. Thus all data complement each other and are essential in determining the complete momentum spectrum. However, in order to take full advantage of all available data from different experiments with completely different experimental setup, care must be taken in their relative normalization. We have chosen the data of Dekkers et al., as the standard of normalization.

The experiment of Baker et al. and that of Fitch et al. were performed with an internal target of which the efficiency was quoted as $\eta = 50 \pm 10\%$. Considering the momentum dependence of the target efficiency, we assumed $\eta = 50$, 53 and 60% at $P_i = 10.9$, 20.9 and 30.9 and 33.9 BeV/c respectively. Because of the uncertainties of these efficiencies and the uncertainties of the effect of the AGS fringe field on the secondary particles, relatively large errors (20%) were assigned to the experimental data. Whether further normalization relative to the data of Dekkers et al. is necessary or not will be found in the least square analysis.

The normalization of the data of Lundy et al. was checked in two ways. First, the forward production spectra of $\pi^{\pm}$ and protons at 13.4 BeV/c were obtained by extrapolating the data to zero degree, and were then compared with the corresponding forward production spectra of Dekkers et al. at 11.8, 18.8 and 23.1 BeV/c. Secondly, various normalization factors were assumed and least square analyses were carried out with all other experimental data ranging from 11 to 34 BeV/c. Both results are consistent with a normalization factor of 1.5 to be multiplied to the data of Lundy et al. The errors assigned to these data in the least square analysis were 15%.

In converting the unit from (mb/nucleus) to (number of pions/interacting proton), the absorption cross section σ_a was taken to be 227 mb[5]. To summarize, the data from different experiments were normalized and the units were converted by

$$\frac{d^2N}{d\Omega dp} \quad \text{(number of pions/sr/BeV/c/interacting proton)}$$

$$= \frac{N_L}{\sigma_a} \left(\frac{d^2\sigma}{d\Omega dp}\right)_{\text{Lundy et al.}} \quad \text{(mb/sr/BeV/c/nucleus)} \qquad (6)$$

$$= \frac{1}{\sigma_a} \left(\frac{d^2\sigma}{d\Omega dp}\right)_{\text{Dekkers et al.}} \quad \text{(mb/sr/BeV/c/nucleus)}$$

$$= \frac{N_B}{\eta} \left(\frac{d^2N}{d\Omega dp}\right)_{\substack{\text{Baker et al.} \\ \text{Fitch et al.}}} \quad \text{(number of pions/sr/BeV/c/circulating proton)}$$

where N_L (=1.5) and N_B are the normalization factors for the data of respective authors, and η_i is the efficiency of the internal target. N_B turned out to be $\sim$ 1 with the choice of η_i mentioned before.

B. Least Square Analysis

The Fortran program "LEAST"[6] was used to determine the parameters C_1 through C_8 and m, by minimizing the quantity

$$Q = \frac{1}{F} \sum_i \left[\frac{\log \left(\frac{d^2N}{d\Omega dp}\right)^e_i - \log \left(\frac{d^2N}{d\Omega dp}\right)^c}{\Delta\left(\frac{d^2N}{d\Omega dp}\right)^e_i \Big/ \left(\frac{d^2N}{d\Omega dp}\right)^e_i} \right]^2 \qquad (7)$$

where the superscript e and c refer to the experimental and calculated values respectively, $\Delta \left(\frac{d^2N}{d\Omega dp}\right)^e_i$ is the error pertaining to the i-th experimental datum and F is the number of degrees of freedom in the least square fitting. Good fits were obtained for both π^+ and π^- data with m consistent with 1. Consequently m was set to 1 and equally good fits were obtained with the following parameters.

	C_1	C_2	C_3	C_4	C_5	C_6	C_7	C_8	data	Q
π^+	1.092	.6458	4.046	1.625	1.656	5.029	.1722	82.65	134	0.72
π^-	0.821	.5271	3.956	1.731	1.617	4.735	.1984	88.75	152	0.73

The calculation was done by CDC-6600 and the results were plotted by the CAL-COMP plotter by means of the Fortran program "YIELD" written for this purpose. They are reproduced in Fig. 2 through Fig. 19. The fact that no normalization for the data of Baker et al. was necessary indicates that our assignment of the target efficiency is probably not far from reality.

4. Multiplicities, Mean Secondary and Transverse Momenta, and Inelasticities.

In addition to the momentum spectra, an important experimental observable

that can provide a direct check to the validity of the formula is the pion multiplicities N_π, defined by

$$N_\pi = \int_0^{P_i} \int_0^{\pi} 2\pi \frac{d^2N}{d\Omega dp} \sin\theta d\theta dp \qquad (8)$$

Other quantities of interest are the mean secondary momentum $\bar{p}$, mean transverse momentum P_t and the inelasticities K_π defined respectively by

$$\bar{p} = \frac{1}{N_\pi} \int_0^{P_i} \int_0^{\pi} 2\pi \frac{d^2N}{d\Omega dp} p \sin\theta d\theta dp \qquad (9)$$

$$P_t = \frac{1}{N_\pi} \int_0^{P_i} \int_0^{\pi} 2\pi \frac{d^2N}{d\Omega dp} p \sin^2\theta d\theta dp \qquad (10)$$

and

$$K_\pi = \frac{1}{P_i} \int_0^{P_i} \int_0^{\pi} 2\pi \frac{d^2N}{d\Omega dp} p \sin\theta d\theta \qquad (11)$$

The integrations were carried out numerically, and the results are presented in Table I. A comparison of the calculated multiplicities with the experimental measurements is given in Table II (Section 5).

Table I - Pion Multiplicities, Mean Secondary and Transverse Momentum, and Inelasticities Predicted by the Proposed Formula.

	P_i (BeV/c)	N_π	$\bar{p}$	P_t	K_π
π^+	10	0.97	0.82	0.23	.080
	15	1.17	1.14	0.24	.089
	20	1.38	1.46	0.25	.101
	25	1.64	1.77	0.26	.116
	30	1.94	2.06	0.27	.134
	35	2.33	2.32	0.28	.155
π^-	10	0.87	0.70	0.22	.061
	15	1.02	0.95	0.24	.065
	20	1.18	1.22	0.25	.072
	25	1.37	1.50	0.25	.082
	30	1.61	1.77	0.26	.095
	35	1.91	2.02	0.27	.111

5. Discussion and Comments on Previous Formulas

One interesting feature the present analysis revealed is that the power to the production angle θ reduced to one after the least square fitting, despite some indications of the necessity of higher powers called for by various authors.[7,8,9] Furthermore, the coefficient for the term $P\theta$ is independent of the incident momentum. Therefore, in conjunction with the cosmic ray results at higher energies, it can be considered as established that the transverse momentum distribution of secondary pions is independent of the incident proton momentum P_i for $P_i > 10$ BeV/c.

Several empirical formulas for pion productions have so far been proposed. The formula due to Cocconi, Koester and Perkins[10] assumes a Boltzman distribution for the transverse momentum, and a simple exponential for the forward energy spectrum. It is attractive with its elegant and simple assumptions. However, the representation is fairly qualitative between 10 and 34 BeV/c. It is perhaps of special use at higher energies. Von Dardel's formula[7] is also rather qualitative. The formula due to Haberler[11] is reasonably quantitative, but the parameters are discontinuous. The formula of Burns et al.[8] gives good representation at 20 and 30 BeV only with different parameters, therefore, is not suitable for general purpose. Trilling's formula[12] is based on an attractive combination of the philosophies of the statistical and isobar models and presents very impressive bumps on the momentum spectrum at higher energies; however, it still remains relatively qualitative below 30 BeV. A step toward a quantitative representation between 10 and 30 BeV was recently presented by Ranft by means of a ten-parameter formula, yet the prediction of the pion multiplicities still remains quite poor.

A comparison of the predictions of the pion multiplicities from three most recent formulas with the experimental measurements is presented in Table II.

Table II - A Comparison of the Measured and Predicted Pion Multiplicities, $N_{\pi^+} + N_{\pi^-}$.

P_i (BeV/c)	Experiment*	Proposed Formula	Ranft Formula*	Trilling Formula*
10	1.9 - 2.3	1.84	0.82	0.72
15	2.5	2.19	1.32	0.85
20		2.56	1.85	0.95
25	2.9 - 3.7	3.01	2.39	1.04
30		3.55	2.94	1.12

*These items are quoted from Reference 9.

6. Conclusion

Aside from the goodness of fits to the momentum spectrum, the most remarkable achievement of the present formula is perhaps its excellent prediction of the pion multiplicities, with which the previous formulas really did not have much luck. It is conceivable, therefore, that the present formula is definitely more realistic than any hitherto available formulas as far as the quantitative representation of the pion flux from P-Be collision between 10 and 35 BeV/c incident momenta is concerned. Further study and some modification of the formula may enable an extrapolation to a higher energy. Similar study on kaon and antiproton production is quite promising, and the results will appear in Part II of this report before long.

We appreciate Miss Janet Head for programming "YIELD" and other assistances. One of us (CLW) thanks Dr. Rudolph Sternheimer and Dr. George Trilling for useful conversations. The effort of Mr. Fred Kuehl, Mr. Paul Hallowell and Mr. Malcolm McCrum in various stages of the data reduction and analysis is gratefully acknowledged.

JRS/CLW:lsl
Distr: B1, B2, B3

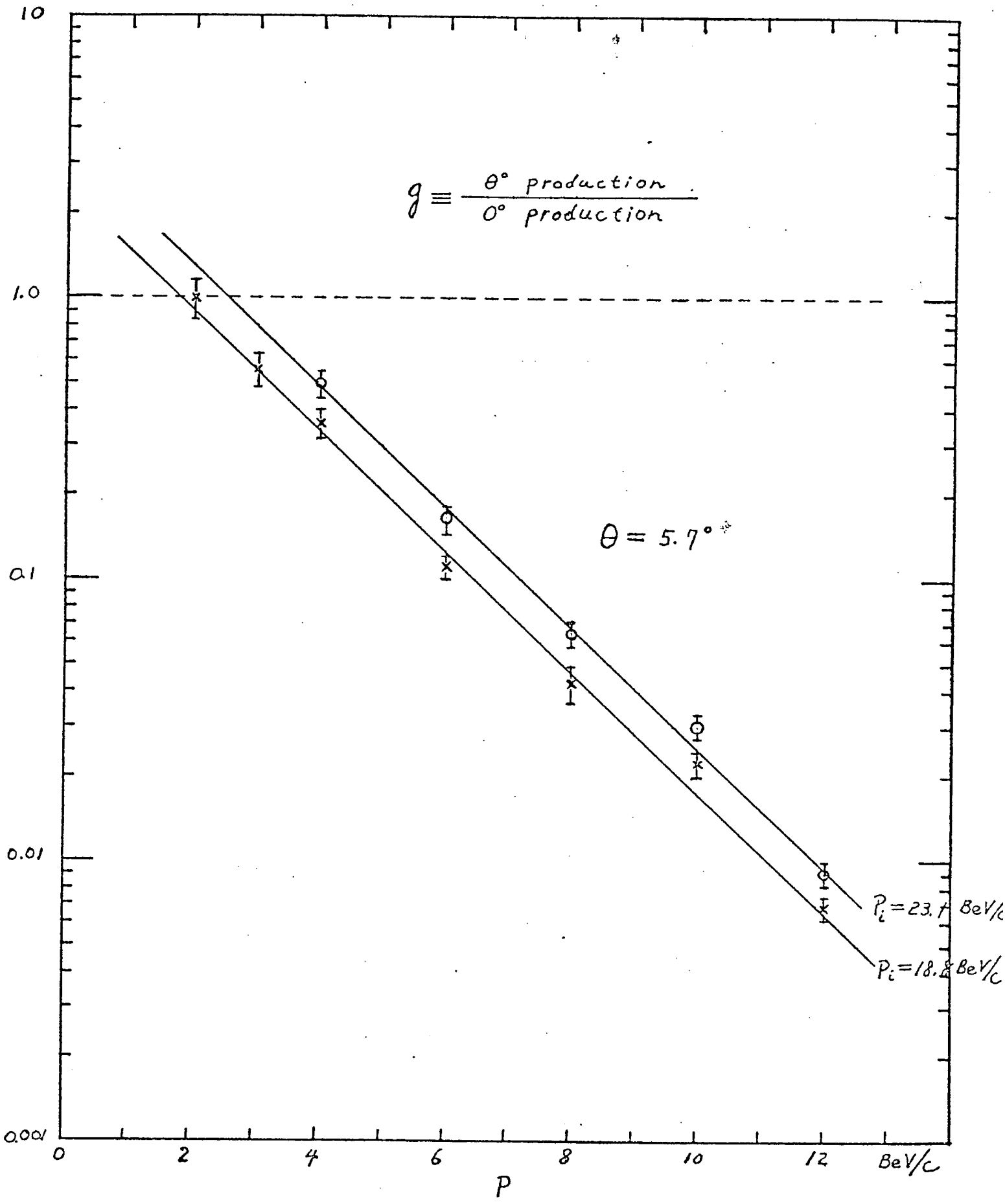
g(θ, P, Pi)
10
1.0
0.1
0.01
0.001
g ≡ θ° production / 0° production
θ = 5.7°
Pi = 23.1 BeV/c
Pi = 18.8 BeV/c
0
2
4
6
8
10
12
BeV/c
P

Fig. 1